Scuola di Fisica Nucleare Raimondo Anni

Secondo corso

Transizioni di fase liquido-gas nei nuclei

Maria Colonna LNS-INFN Catania

Otranto, 29 Maggio-3 Giugno 2006

Chomaz,Colonna,Randrup Phys. Rep. 389(2004)263
Baran,Colonna,Greco,DiToro Phys. Rep. 410(2005)335

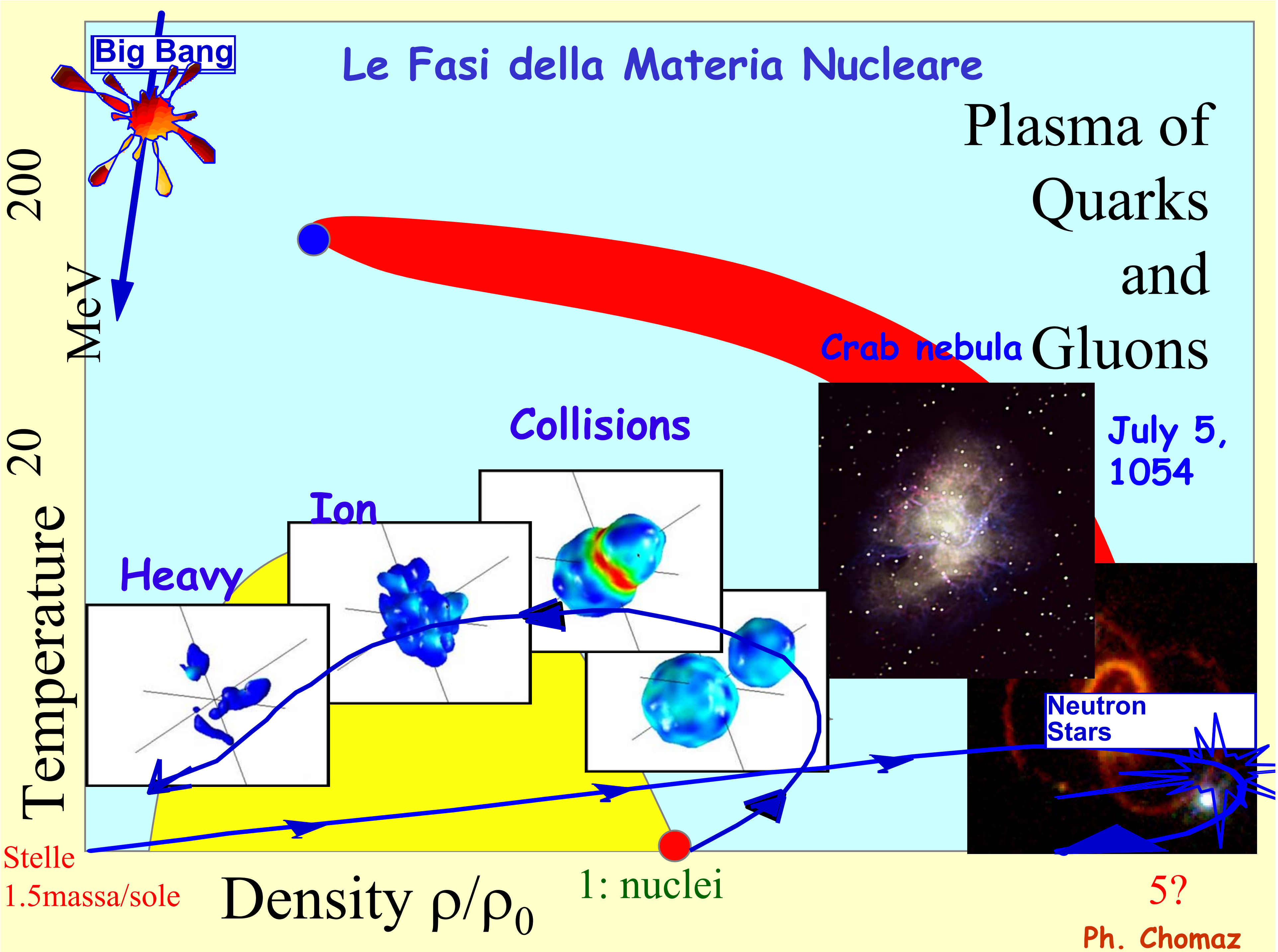

Le Fasi della Materia Nucleare
Big Bang
Plasma of Quarks and Gluons
Crab nebula
July 5, 1054
Collisions
Ion
Heavy
Neutron Stars
200
20
MeV
Temperature
Stelle 1.5massa/sole
Density ρ/ρ_0
1: nuclei
5?
Ph. Chomaz

Osservazione sperimentale:

frammentazione nucleare,
rivelazione di frammenti di massa intermedia (IMF)
in collisioni fra ioni pesanti alle energie di Fermi
(30-80 MeV/A)

Obiettivi:

- stabilire connessione con transizione di fase liquido-gas, determinare diagramma di fase di materia nucleare
Termodinamica della transizione di fase in sistemi finiti

- studiare il meccanismo di frammentazione e individuare osservabili che vi siano legate per ottenere informazioni sul comportamento a bassa densita' delle forze nucleari.
Ex: osservabili cinematiche, massa, N/Z degli IMF

- Transizioni di fase liquido-gas
  e segnali associati

- Meccanismi di frammentazione
  Dinamica nucleare nella zona di co-esistenza
  Moti collettivi instabili, instabilita' spinodale

- Approcci dinamici per sistemi nucleari

- Frammentazione in collisioni centrali e periferiche

- Ruolo del grado di liberta' di isospin

Phase co-existence

$$S([\boldsymbol{X}_1, \boldsymbol{X}_2, \ldots]) = \sum_i S_i(\boldsymbol{X}_i)$$

Entropy S

X, extensive variables: Volume, Energy, N

$$0 \doteq \sum_i \delta S_i(\boldsymbol{X}_i = \bar{\boldsymbol{X}}_i) = \sum_{i\ell} \left(\frac{\partial S_i}{\partial X_i^\ell}\right)_{\boldsymbol{X}_i = \bar{\boldsymbol{X}}_i} \delta X_i^\ell = \sum_{i\ell} \lambda_i^\ell \, \delta X_i^\ell$$

$$\lambda_i^E \equiv \frac{\partial S_i}{\partial E_i} = \frac{1}{T_i}, \quad \lambda_i^N \equiv \frac{\partial S_i}{\partial N_i} = -\frac{\mu_i}{T_i}, \quad \lambda_i^V \equiv \frac{\partial S_i}{\partial V_i} = \frac{P_i}{T_i}$$

λ, intensive variables: temperature, pressure, chemical potential

Stability conditions

$$0 \dot{>} \sum_i \delta^2 S_i^\prime (\mathbf{X}_i = \bar{\mathbf{X}}_i) = \sum_{i\ell\ell'} \left(\frac{\partial^2 S_i^\prime}{\partial X_i^\ell \partial X_i^{\ell'}} \right)_{\mathbf{X}_i = \bar{\mathbf{X}}_i} \delta X_i^\ell \delta X_i^{\ell'}$$

$$EE \quad : \quad 0 > \frac{\partial \lambda^E}{\partial E} = -\frac{1}{T^2} \frac{\partial T}{\partial E} \Rightarrow C \equiv \frac{\partial E}{\partial T} > 0$$

$$VV \quad : \quad 0 > \frac{\partial \lambda^V}{\partial V} = \frac{1}{T} \frac{\partial P}{\partial V} \Rightarrow \kappa^{-1} \equiv -V \frac{\partial P}{\partial V} > 0 \, ,$$

$$NN \quad : \quad 0 > \frac{\partial \lambda^N}{\partial N} = -\frac{1}{T} \frac{\partial \mu}{\partial N} \Rightarrow \chi^{-1} \equiv \frac{\partial \mu}{\partial N} > 0 \, .$$

Maxwell construction

$$\tilde{S} = N_1\sigma(x_1) + N_2\sigma(x_2) = \frac{N_1}{N}S(X_1) + \frac{N_2}{N}S(X_2) > S$$

$$\int_{X_1}^{X_2} dX \, (\lambda(X) - \lambda_0) \doteq 0$$

λ pressure, X volume

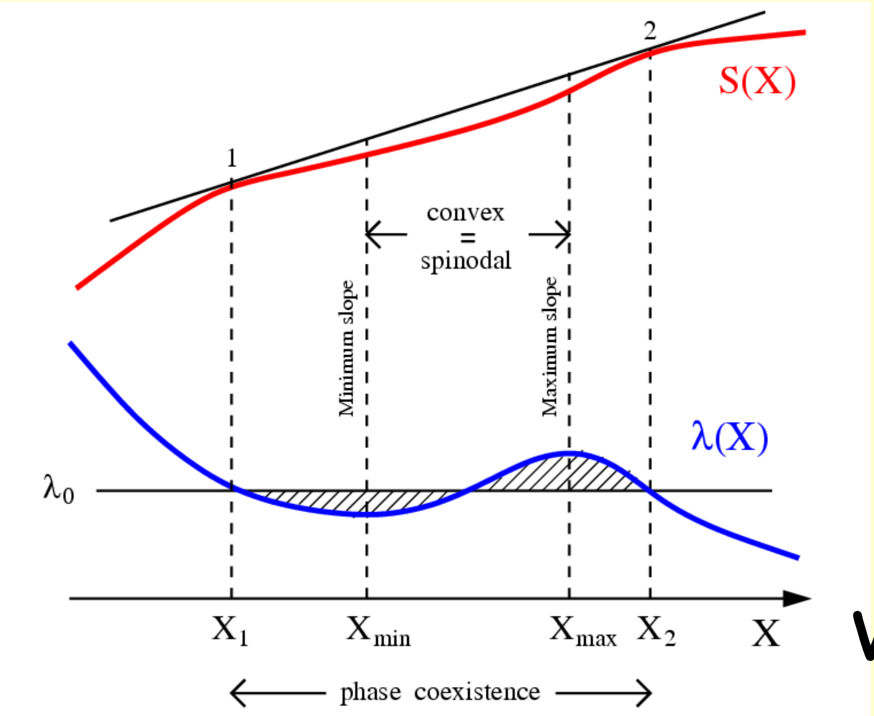

V

Spinodal instabilities are directly connected to first-order phase transitions and phase co-existence: a good candidate as fragmentation mechanism

$$S_i(\boldsymbol{X}_i) \;\rightarrow\; S'_i(X_i^{\ell}, \lambda^{\ell'}) \equiv S_i(\boldsymbol{X}_i) - {\sum_{\ell'}}' \lambda^{\ell'} X_i^{\ell'}$$

Canonical ensemble

$$S' = S - E/T$$

$$-TS' = \bar{E} - TS = V f(T, \rho).$$

F (free energy)

$$P(T;N,V) \;=\; -\left(\frac{\partial F}{\partial V}\right)_{TN} \;=\; \frac{NT}{V-bN} - a\left(\frac{N}{V}\right)^2 \;=\; \frac{\rho T}{1-b\rho} - a\rho^2$$

Mean-field approximation

From the Van der Waals gas

to

Nuclear Matter phase diagram

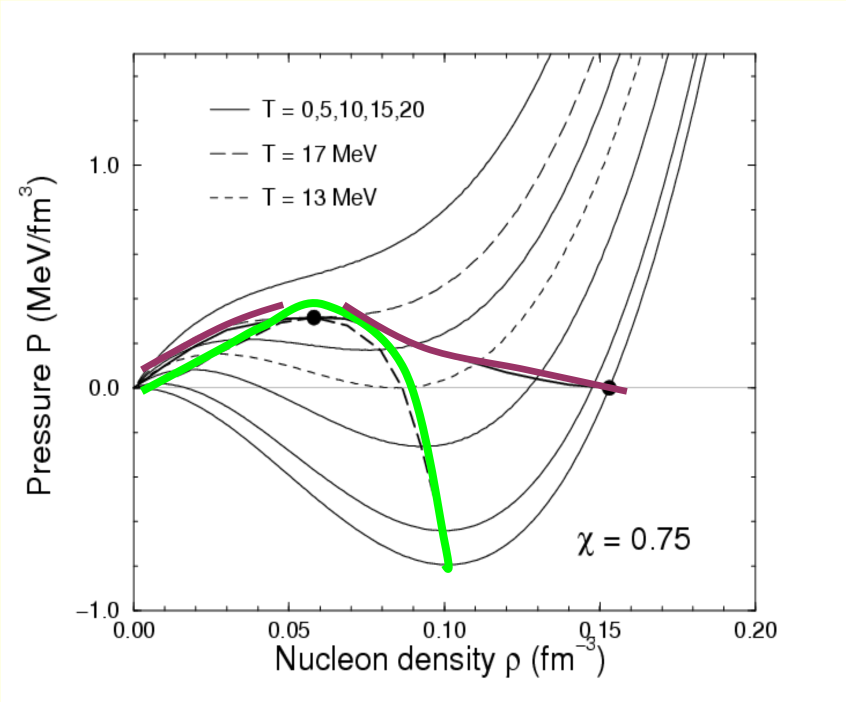

$$V_{12} \;=\; \delta(\boldsymbol{r}_1 - \boldsymbol{r}_2)\left(t_0 + \tfrac{1}{6} t_3 \rho\left(\frac{\boldsymbol{r}_1 + \boldsymbol{r}_2}{2}\right)^{\sigma}\right)$$

$t_0 < 0$, $t_3 > 0$ ⟶ $F(\rho)$

$$\kappa^{-1} \equiv -V\frac{\partial P}{\partial V} = \rho \frac{\partial P}{\partial \rho} < 0$$ ⟶ instabilities

Phase diagram for classical systems

$$\dot{\boldsymbol{r}}_i = \frac{\partial H}{\partial \boldsymbol{p}_i} \ , \ \dot{\boldsymbol{p}}_i = -\frac{\partial H}{\partial \boldsymbol{r}_i} \ , \ i = 1, \ldots, A \ .$$

$$T \ = \ \frac{1}{3A} \sum_i \boldsymbol{p}_i \cdot \frac{\partial H}{\partial \boldsymbol{p}_i} \ = \ \frac{1}{3A} \sum_i \boldsymbol{p}_i \cdot \dot{\boldsymbol{r}}_i \ .$$

$$P \ = \ \mathrm{trc}\, \boldsymbol{T} \ = \ \rho \left(T + \frac{1}{A} \sum_{i<j} F_{ij} r_{ij} \right)$$

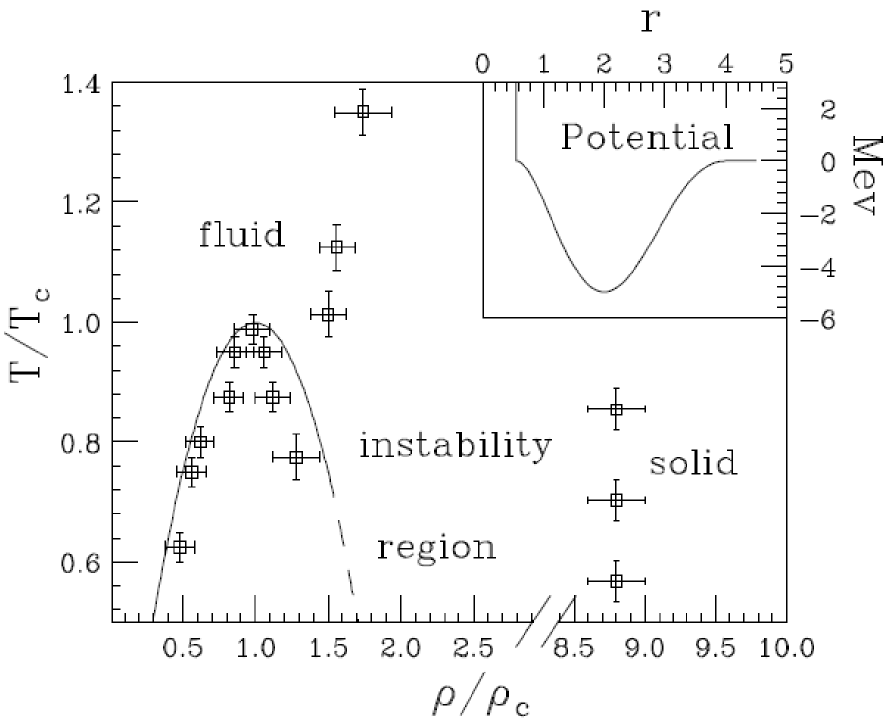

Two – component fluids (neutrons and protons)

$$F(T,V,N_p,N_n) = \quad V f(T,\rho_p,\rho_n)$$

$$\left(\frac{\partial P}{\partial \rho} = \rho \frac{\partial \mu}{\partial \rho} \right)$$

$$\mu_n \equiv \frac{\partial F}{\partial N_n} = \frac{\partial f}{\partial \rho_n}\ , \quad \mu_p \equiv \frac{\partial F}{\partial N_p} = \frac{\partial f}{\partial \rho_p}$$

$$\boldsymbol{C} = \begin{pmatrix} \partial^2 f/\partial\rho_n\partial\rho_n & \partial^2 f/\partial\rho_p\partial\rho_n \\ \partial^2 f/\partial\rho_n\partial\rho_p & \partial^2 f/\partial\rho_p\partial\rho_p \end{pmatrix} = \begin{pmatrix} \partial\mu_n/\partial\rho_n & \partial\mu_n/\partial\rho_p \\ \partial\mu_p/\partial\rho_n & \partial\mu_p/\partial\rho_p \end{pmatrix}$$

$$\det[\boldsymbol{C}] = c_- c_+ > 0 \quad \text{and} \quad \mathrm{tr}[\boldsymbol{C}] = \mathrm{c}_- + \mathrm{c}_+ > 0$$

$$\left(\frac{\partial \mu_p}{\partial y}\right)_{T,p} \left(\frac{\partial P}{\partial \rho}\right)_{T,y} = (1-y)\rho^2 |\boldsymbol{C}|$$

Chemical inst. Mechanical inst.

Y proton fraction = ρ_p/ρ

Phase co-existence in asymmetric matter

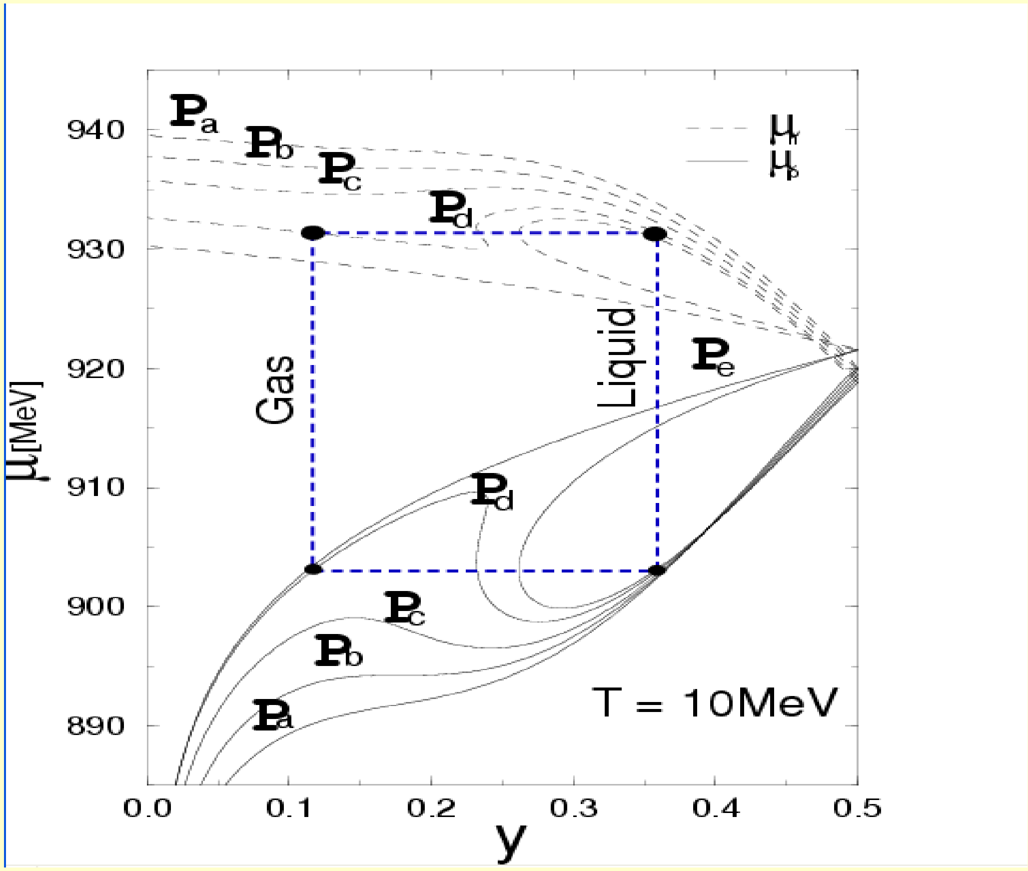

In asymmetric matter phase co-existence happens between phases with different asymmetry:
The iso-distillation effect, a new probe for the occurrence of phase transitions

Phase diagram in asymmetric matter

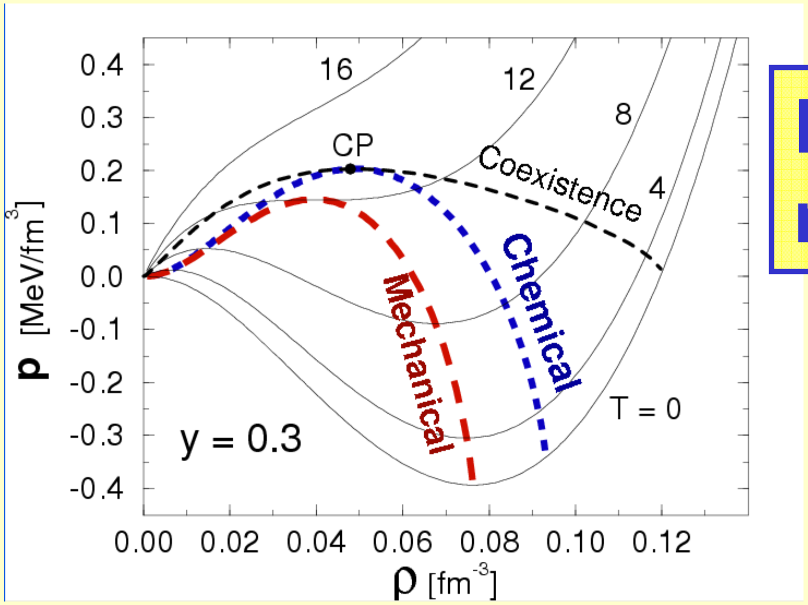

In asymmetric matter phase co-existence happens between phases with different asymmetry:
The iso-distillation effect, a new probe for the occurrence of phase transitions

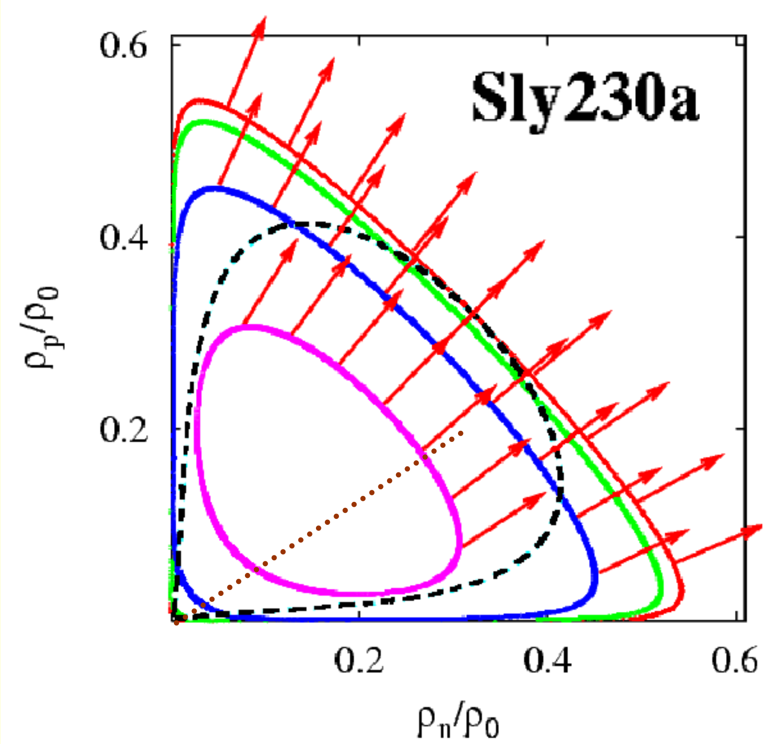

Two-dimensional spinodal boundaries for fixed values of the sound velocity

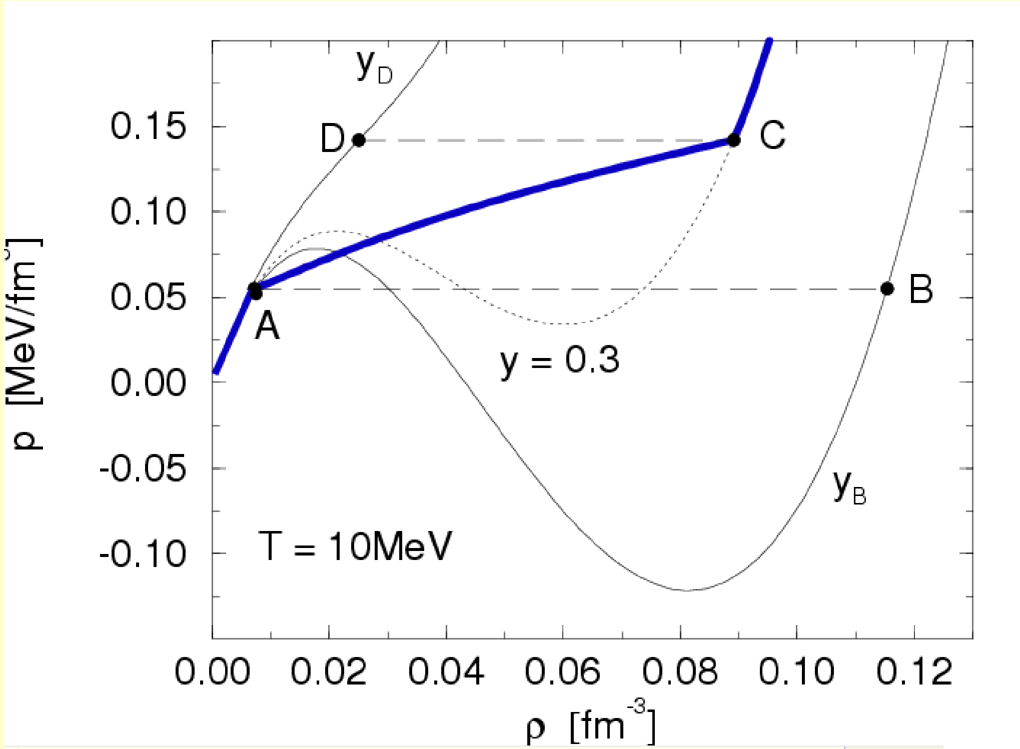

Phase transition in asymmetric matter

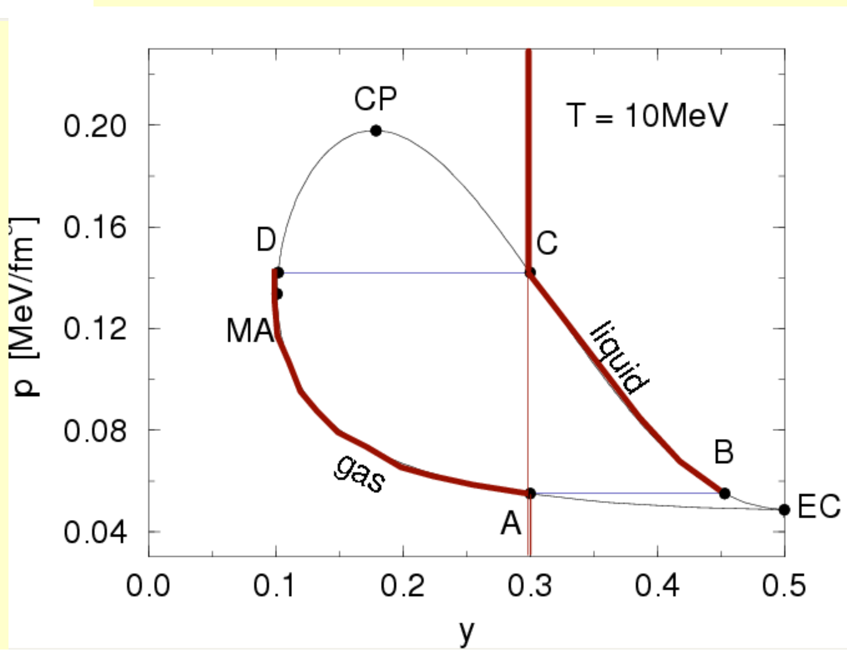

Phase transitions in finite systems

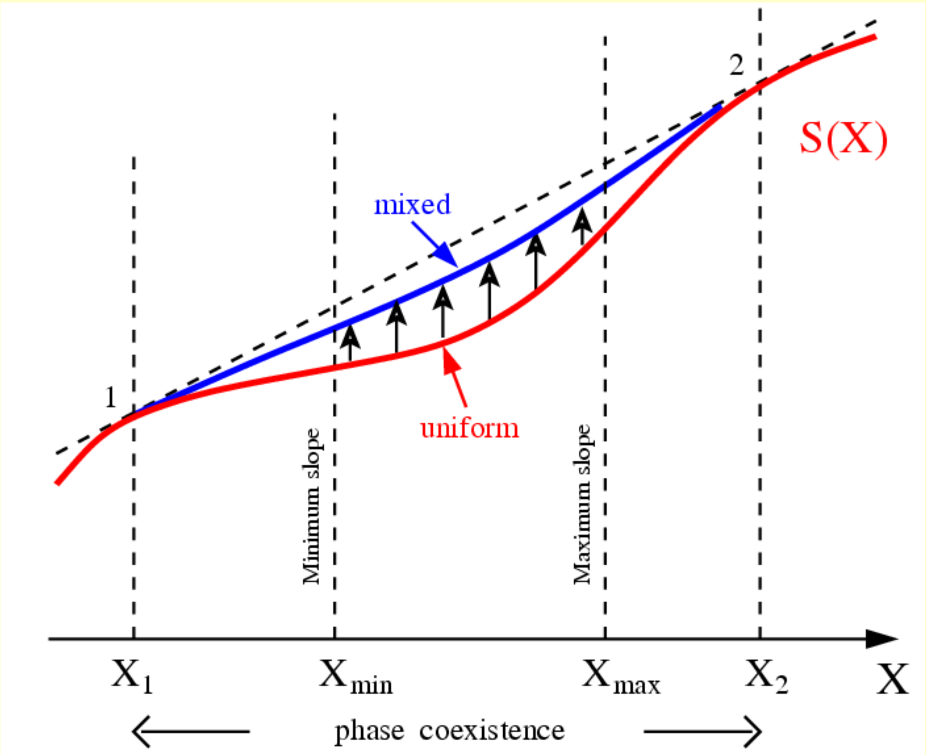

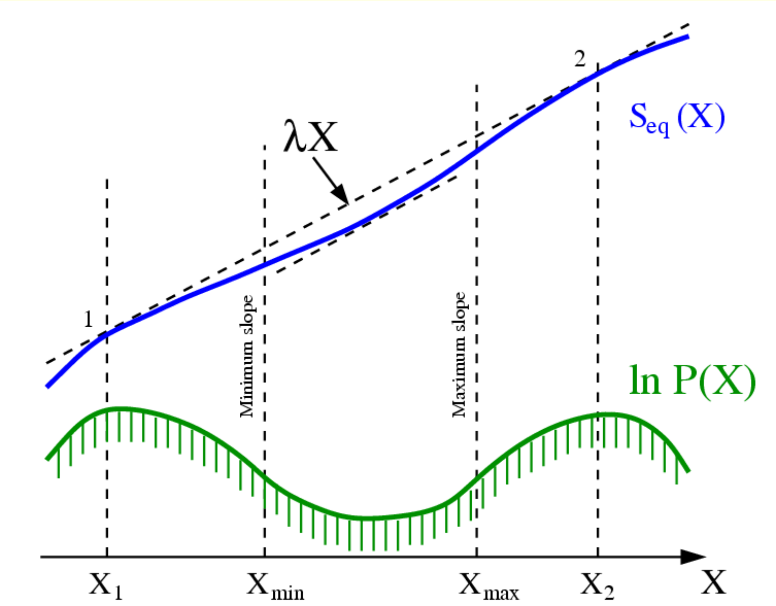

Probability P(X) for a system in contact with a reservoir →

Bimodality, negative specific heat

Lattice-gas canonical ensemble fixed V

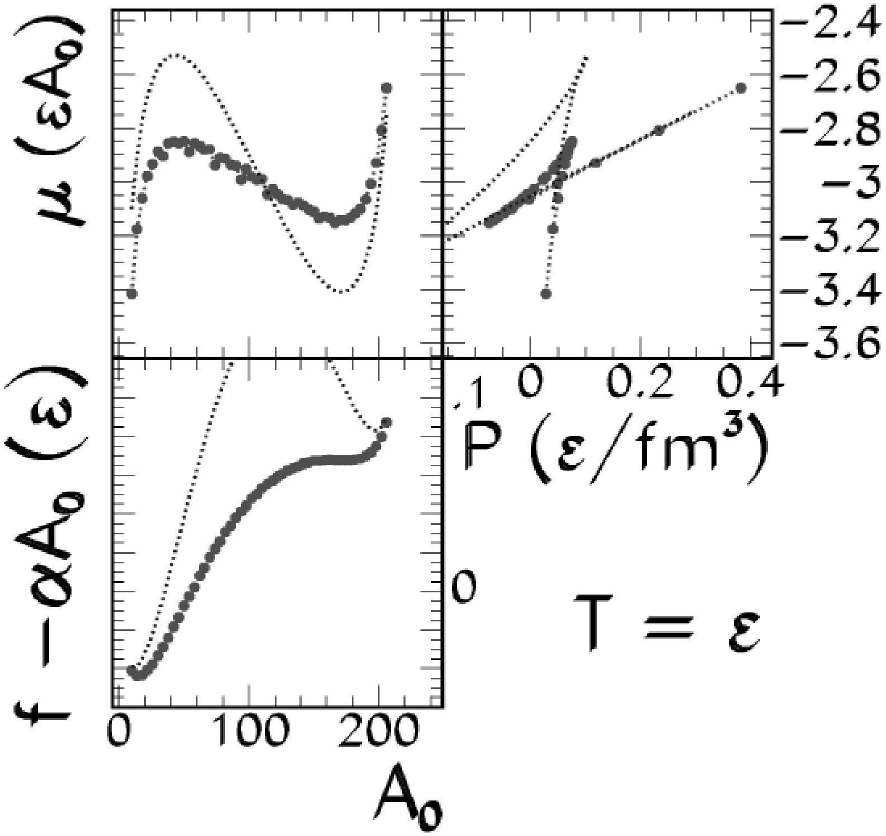

Isochore ensemble

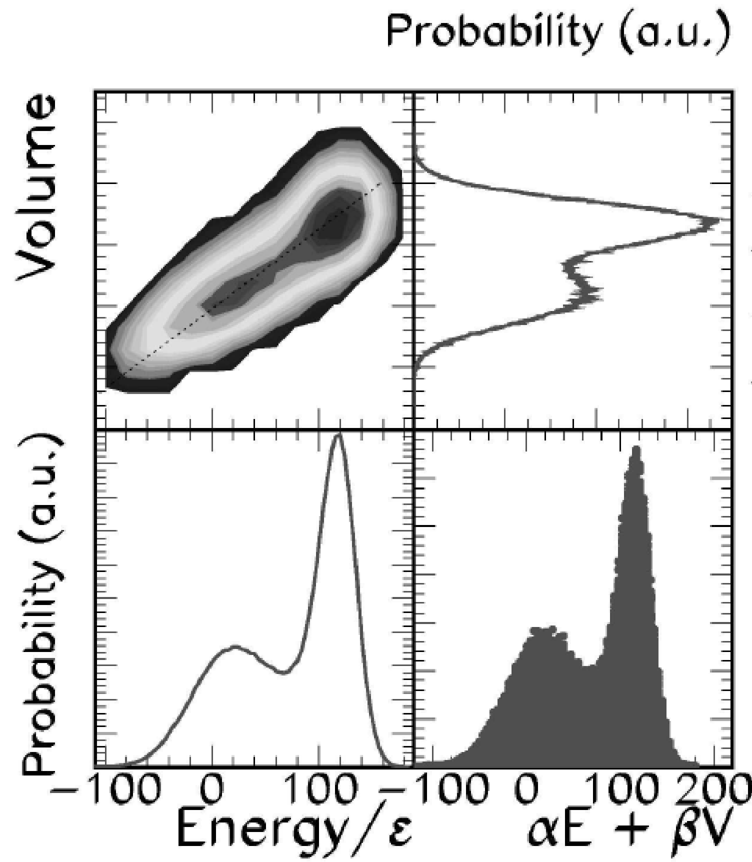

$$S_i(\boldsymbol{X}_i) \;\rightarrow\; S'_i(X_i^{\ell}, \lambda^{\ell'}) \equiv S_i(\boldsymbol{X}_i) - {\sum_{\ell'}}' \lambda^{\ell'} X_i^{\ell'}$$

$$P_{\beta\lambda_v}(E,V) = \bar{W}(E,V) Z_{\beta\lambda_v}^{-1} \mathrm{e}^{-\beta E - \lambda_v V}$$

$$\bar{W}(E,V) = \exp(\bar{S}(E,V))$$

Curvature anomalies and bimodality

Hydrodynamical instabilities in classical fluids

Navier-Stokes equation

$$\frac{d}{dt}\rho\boldsymbol{v} \equiv \frac{\partial}{\partial t}\rho\boldsymbol{v} + \boldsymbol{v}\cdot\boldsymbol{\nabla}\rho\boldsymbol{v} = \boldsymbol{\nabla}P$$

Continuity equation

$$\frac{\partial}{\partial t}\rho + \boldsymbol{\nabla}\cdot\rho\boldsymbol{v} = 0$$

Linearization →

$$\delta\rho(\boldsymbol{r},t) = \rho(\boldsymbol{r},t) - \rho_0,$$

$$\rho_0\partial\boldsymbol{v}/\partial t = \boldsymbol{\nabla}P, \qquad \partial\delta\rho/\partial t = \rho_0\boldsymbol{\nabla}\cdot\boldsymbol{v}.$$

$$\frac{\partial^2}{\partial t^2}\delta\rho(\boldsymbol{r},t) = \nabla^2 P = \left(\frac{\partial P}{\partial\rho}\right)_{\rho=\rho_0}\nabla^2\delta\rho(\boldsymbol{r},t)$$

$$\omega_k^2 = v_s^2k^2 \quad \text{or} \quad k^2 = \rho m\kappa\omega_k^2$$

$$\kappa^{-1} \equiv -V\frac{\partial P}{\partial V} = \rho\frac{\partial P}{\partial\rho}$$

Link between dynamics and thermodynamics !

Collective motion in Fermi fluids

Derivation of fluid dynamics from a variational approach

$$I = \int dt \langle \Psi | i\hbar\partial/\partial t - \hat{H} | \Psi \rangle$$

$$\Psi(\boldsymbol{r}_1, \boldsymbol{r}_2, .., \boldsymbol{r}_A; t) \; = \; \Phi(\boldsymbol{r}_1, \boldsymbol{r}_2, .., \boldsymbol{r}_A; t) \, e^{\frac{i}{\hbar} S(\boldsymbol{r}_1, \boldsymbol{r}_2, .., \boldsymbol{r}_A; t)}$$

Phase S is additive, Φ Slater determinant →

$$I \; = \; \int_{t_1}^{t_2} dt \left[-E[\rho] + \int d^3\boldsymbol{r} \left(S(\boldsymbol{r}) \frac{\partial}{\partial t} \rho(\boldsymbol{r}) - \frac{\rho(\boldsymbol{r})}{2m^*(\boldsymbol{r})} \boldsymbol{\nabla} S(\boldsymbol{r}) \cdot \boldsymbol{\nabla} S(\boldsymbol{r}) \right) \right]$$

E = energy density functional

δI (with respect to S) = 0 →

$$\frac{\partial}{\partial t} \rho(\boldsymbol{r}) \; + \; \boldsymbol{\nabla} \cdot (\boldsymbol{u}(\boldsymbol{r}) \rho(\boldsymbol{r})) \; = \; 0$$

$$\boldsymbol{u} = (1/m^*) \boldsymbol{\nabla} S.$$

For a given collective mode ν…

$$S(\boldsymbol{r},t) = \dot{q}_\nu(t) S_\nu(\boldsymbol{r}) \qquad \delta\rho(\boldsymbol{r},t) = q_\nu(t)\delta\rho_\nu(\boldsymbol{r}),$$

$$\delta\rho_\nu = -\rho_0 \boldsymbol{\nabla}((1/m^*)\boldsymbol{\nabla} S_\nu).$$

$$\langle\psi|H|\psi\rangle = E_0 + \tfrac{1}{2} M_\nu \dot{q}_\nu^2 + \tfrac{1}{2} C_\nu q_\nu^2 \ ,$$

$$M_\nu = \int d^3\boldsymbol{r} \frac{\rho_0}{m^*(\boldsymbol{r})} \boldsymbol{\nabla} S_\nu(\boldsymbol{r}) \cdot \boldsymbol{\nabla} S_\nu(\boldsymbol{r}) > 0 \ ,$$

$$C_\nu = \int d^3\boldsymbol{r} \int d^3\boldsymbol{r}' \left(\frac{\delta^2 E[\rho]}{\delta\rho(\boldsymbol{r})\delta\rho(\boldsymbol{r}')} \right)_0 \delta\rho_\nu(\boldsymbol{r}')\delta\rho_\nu(\boldsymbol{r}) \ ,$$

($\mu = dE/d\rho$)

$$\omega_\nu^2 = C_\nu / M_\nu.$$

Ph.Chomaz et al., Phys. Rep. 389(2004)263
V.Baran et al., Phys. Rep. 410(2005)335

$$\mu_{\rm n} \equiv \frac{\partial F}{\partial N_{\rm n}} = \frac{\partial f}{\partial \rho_{\rm n}} \ , \ \mu_{\rm p} \equiv \frac{\partial F}{\partial N_{\rm p}} = \frac{\partial f}{\partial \rho_{\rm p}}$$

$$P(T;N,V) \ = \ -\left(\frac{\partial F}{\partial V}\right)_{TN}$$

$$\kappa^{-1} \ \equiv -V\frac{\partial P}{\partial V} \ = \ \rho \frac{\partial P}{\partial \rho}$$

$$\left(\frac{\partial P}{\partial \rho} = \rho \frac{\partial \mu}{\partial \rho} \right)$$

$U(\rho)$ = dfpot/dρ mean-field potential

$$F_0^{\rm q_1 q_2}(k) \ = \ N_{\rm q_1}(T)\frac{\delta U_{q_1}}{\delta \rho_{\rm q_2}} \ , \quad {\rm q_1, q_2 = n, p}$$

1 + F0 = N dμ/dρ

The nuclear matter case

Plane waves for Sv

$$\omega_{\boldsymbol{k}}^2 = \frac{\rho_0}{2m^*}(A + Bk^2)k^2$$

$$A = \frac{\partial P}{\partial \rho}$$

$$\gamma_k^\infty = -i\omega_k = -\frac{\hbar}{t_k} = \left(-\frac{1}{3}\frac{m^*}{m}(1+F_0)\right)^{\frac{1}{2}} kV_F$$

Landau parameter F0

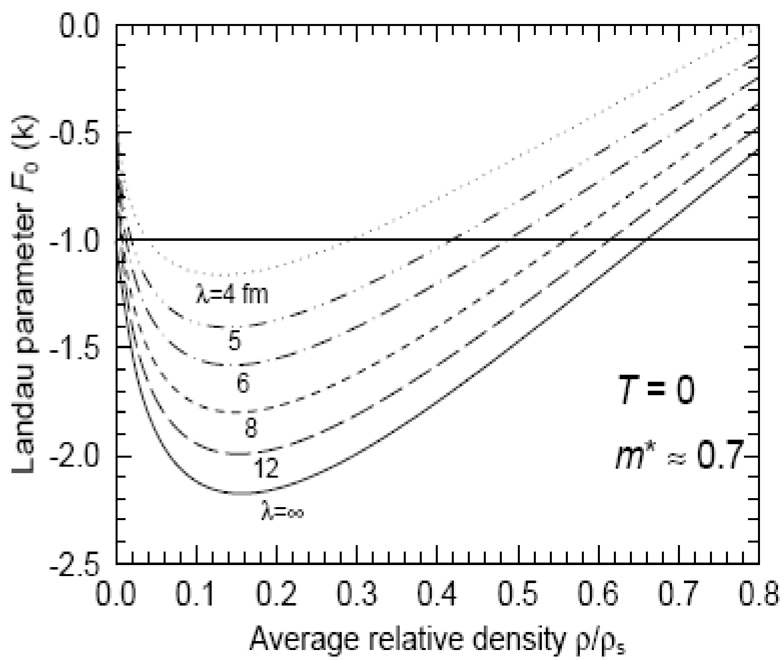

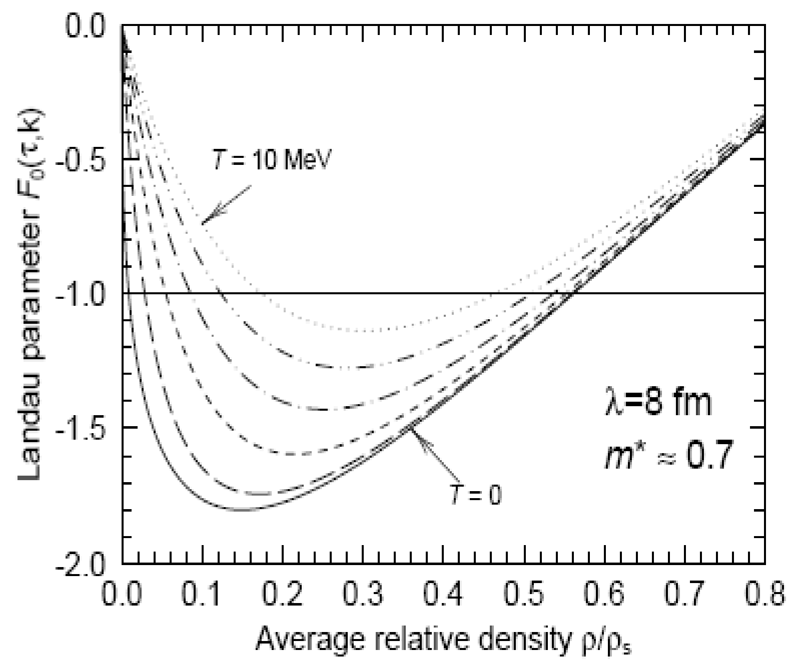

Linearized transport equations: Vlasov

$$\dot{f} \equiv \frac{\partial}{\partial t} f - \{h[f], f\} = 0$$

$$\frac{\partial}{\partial t}\delta f + \frac{\boldsymbol{p}}{m} \cdot \frac{\partial}{\partial \boldsymbol{r}}\delta f - \frac{\partial f_0}{\partial \boldsymbol{p}} \cdot \left(\frac{\partial}{\partial \rho} U \frac{\partial}{\partial \boldsymbol{r}}\delta\rho\right) = 0 \ .$$

U(ρ) = dEpot/dρ **mean-field potential** , (μ = dE/dρ)

f(**r**,**p**,t) one-body distribution function

$$\delta\rho(\boldsymbol{r}, t) = g \int \frac{d^3\boldsymbol{p}}{h^3} \, \delta f(\boldsymbol{r}, \boldsymbol{p}, t)$$

$$\delta f(\boldsymbol{r}, \boldsymbol{p}, t) = \sum_{\boldsymbol{k}} f_{\boldsymbol{k}}(\boldsymbol{p}, t) \, \mathrm{e}^{i\boldsymbol{k}\cdot\boldsymbol{r}}$$

$$f_{\boldsymbol{k}}(\boldsymbol{p}, t) = f_{\boldsymbol{k}}(\boldsymbol{p})\mathrm{e}^{-i\omega_k t}$$

$$(-\omega_k + \boldsymbol{v}\cdot\boldsymbol{k}) f_{\boldsymbol{k}}(\boldsymbol{p}) = \boldsymbol{v}\cdot\boldsymbol{k} \, \frac{\partial f_0}{\partial \epsilon}\frac{\partial U}{\partial \rho} \, \rho_{\boldsymbol{k}}$$

$$0 = \varepsilon(\omega_k) \equiv 1 - \left(g \int \frac{d^3\boldsymbol{p}}{h^3} \frac{\boldsymbol{v}\cdot\boldsymbol{k}}{\boldsymbol{v}\cdot\boldsymbol{k} - \omega_k} \frac{\partial f_0}{\partial \epsilon}\right) \frac{\partial U}{\partial \rho}$$

$$= 1 - \left(g \int \frac{d^3\boldsymbol{p}}{h^3} \frac{(\boldsymbol{v}\cdot\boldsymbol{k})^2}{(\boldsymbol{v}\cdot\boldsymbol{k})^2 - \omega_k^2} \frac{\partial f_0}{\partial \epsilon}\right) \frac{\partial U}{\partial \rho} \ .$$

Dispersion relation in nuclear matter

$$\partial_\rho U \approx \tfrac{2}{3}\epsilon_F F_0/\rho$$

$$\frac{s}{2}\ln\left(\frac{s+1}{s-1}\right) = 1+\frac{1}{F_0}\,.$$

$s = \omega/kv_F$

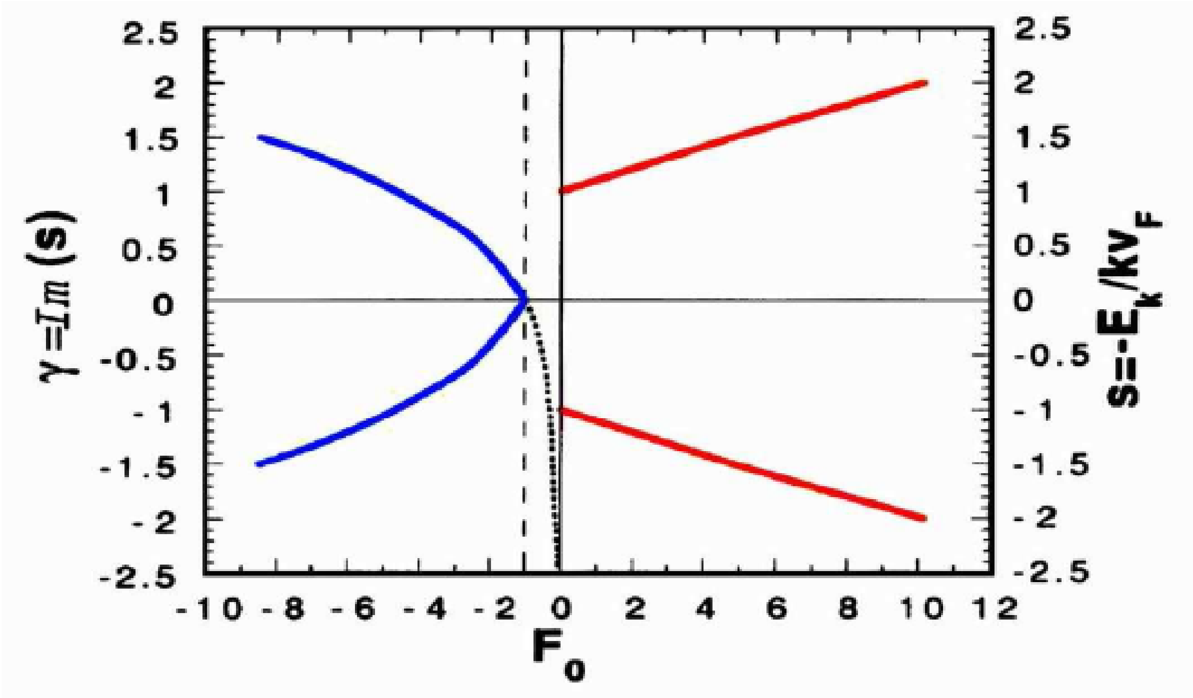

Growth time and dispersion relation

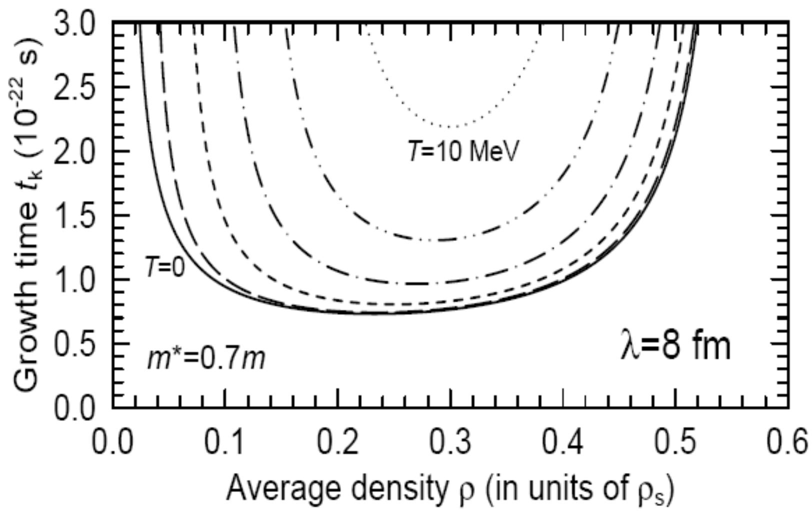

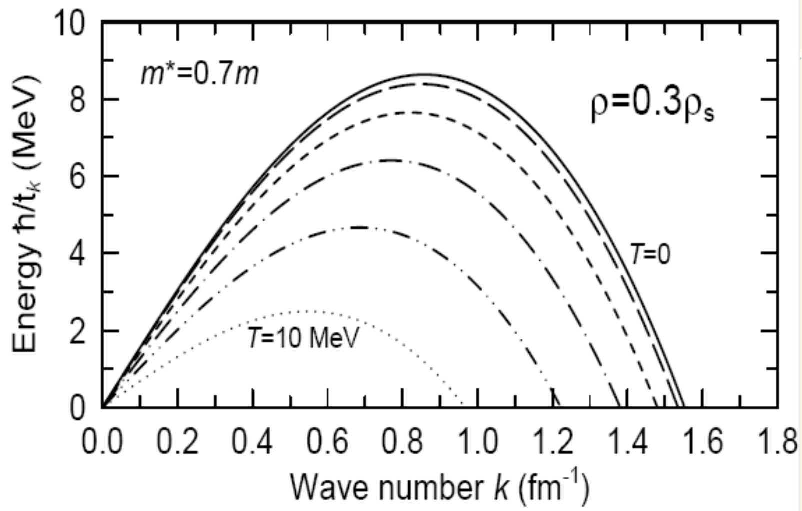

Instability diagram

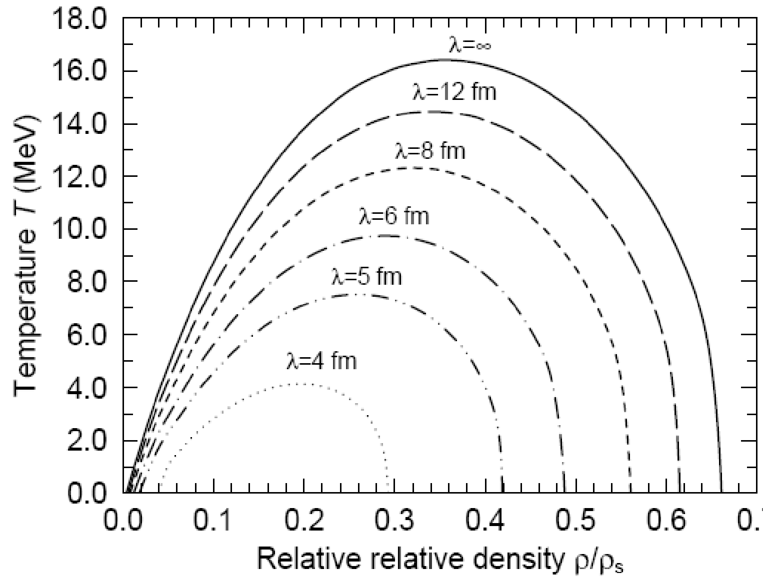

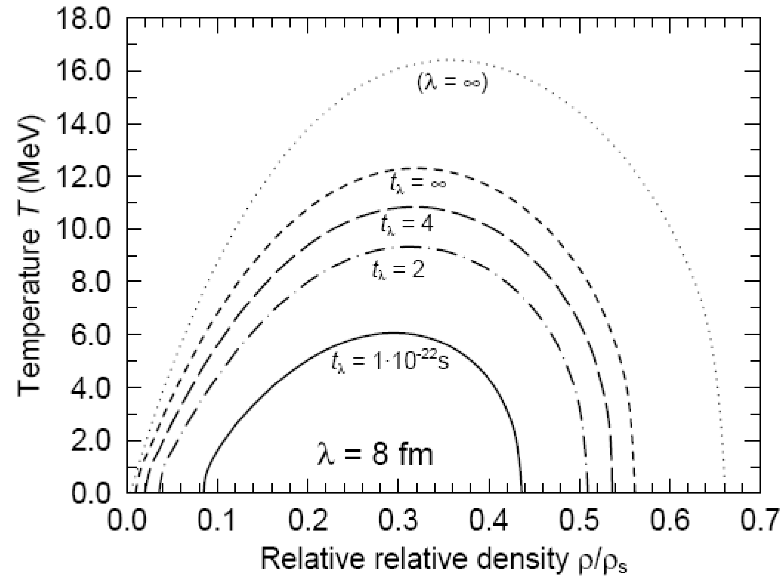

Two-component fluids

$$\frac{\partial}{\partial t}\delta f + \frac{\boldsymbol{p}}{m}\cdot\frac{\partial}{\partial \boldsymbol{r}}\delta f - \frac{\partial f_0}{\partial \boldsymbol{p}}\cdot\left(\frac{\partial}{\partial\rho}U\frac{\partial}{\partial \boldsymbol{r}}\delta\rho\right) = 0 .$$

$$U_{\rm q} = A\left(\frac{\rho}{\rho_0}\right) + B\left(\frac{\rho}{\rho_0}\right)^{\alpha+1} + C\left(\frac{\rho'}{\rho_0}\right)\tau_q + \frac{1}{2}\frac{dC(\rho)}{d\rho}\frac{(\rho')^2}{\rho_0} - D\triangle\rho + D'\tau_{\rm q}\triangle\rho'$$

$\rho' = \rho_n - \rho_p$

τ = 1 neutrons, -1 protons

$$\begin{aligned}
[1 + F_0^{\rm nn}\chi_{\rm n}]\delta\rho_{\rm n} \;+\; [F_0^{\rm np}\chi_{\rm n}]\delta\rho_{\rm p} &= 0 ,\\
[F_0^{\rm pn}\chi_{\rm p}]\delta\rho_{\rm n} \;+\; [1 + F_0^{\rm pp}\chi_{\rm p}]\delta\rho_{\rm p} &= 0 ,
\end{aligned}$$

$$\chi_{\rm q}(\omega,\boldsymbol{k}) = \frac{2}{N_{\rm q}(T)}\int\frac{d^3\boldsymbol{p}}{h^3}\frac{\boldsymbol{k}\cdot\boldsymbol{v}}{\omega + i0 - \boldsymbol{k}\cdot\boldsymbol{v}}\frac{\partial f_{\rm q}^{(0)}}{\partial\epsilon_{\boldsymbol{p}}^{\rm q}} ,$$

$$N_{\rm q}(T) = -2\int\frac{d^3\boldsymbol{p}}{h^3}\frac{\partial f_{\rm q}^{(0)}}{\partial\epsilon_{\boldsymbol{p}}^{\rm q}}$$

$$F_0^{\rm q_1q_2}(k) = N_{\rm q_1}(T)\frac{\delta U_{q_1}}{\delta\rho_{\rm q_2}} , \quad {\rm q_1, q_2 = n, p}$$

Dispersion relation

$$(1+F_0^{nn}\chi_n)(1+F_0^{pp}\chi_p) - F_0^{np}F_0^{pn}\chi_n\chi_p = 0 .$$

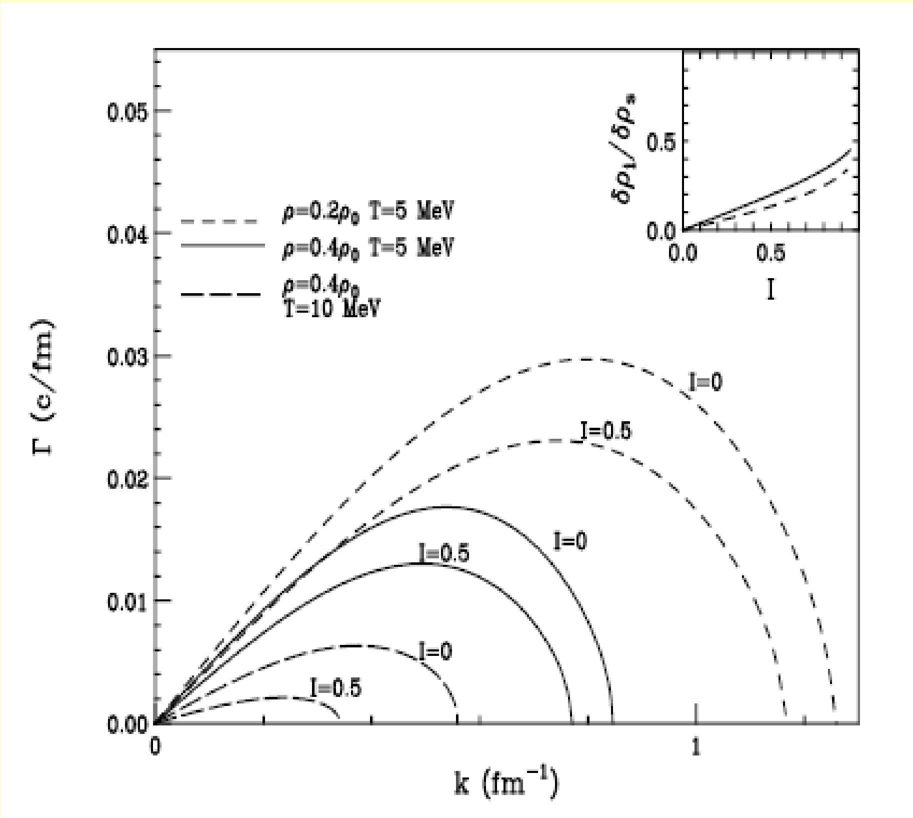

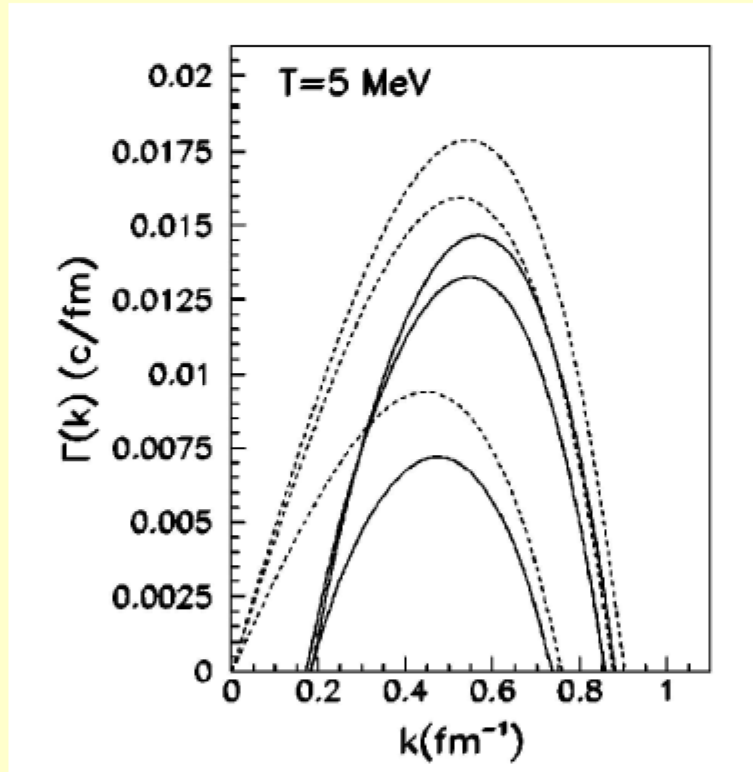

A new effect: Isospin distillation dρp/dρn >ρp/ρn

The liquid phase is more symmetric (as seen in phase co-existence)

Finite nuclei

$$\left[h[\rho_0] - \lambda\hat{Q}, \rho_0\right] = 0$$

$$\rho'(t) \equiv e^{\frac{i}{\hbar}\lambda\hat{Q}t} \rho(t) e^{-\frac{i}{\hbar}\lambda\hat{Q}t}$$

$$i\hbar\frac{\partial}{\partial t}\rho'(t) = [h'(t) - \lambda\hat{Q}, \rho'(t)]$$

Linearized Schroedinger equation (RPA) for dilute systems

α = density dilution

$$i\hbar\frac{\partial}{\partial t}\delta\rho' = [h'_0(t) - \lambda Q', \delta\rho'] + [\delta U'(t), \rho'_0(t)] = \mathcal{M}(t)\cdot\delta\rho'(t)$$

$$(\hbar\omega_\nu - \epsilon_i + \epsilon_j)\langle i|\delta\rho_\nu|j\rangle = (\rho_j - \rho_i)\langle i|\delta U_\nu|j\rangle$$

$$\omega_\nu\rho_\nu^{ij} = (\epsilon_i - \epsilon_j)\rho_\nu^{ij} + \sum_{kl}(n_j - n_i)V_{il,kj}\rho_\nu^{kl} .$$

$$n'_i = [1 + \exp((\varepsilon_i - \varepsilon_F(\alpha^2 T))/\alpha^2 T)]^{-1}, \quad \langle r|R(\alpha)\varphi\rangle = \alpha^{-\frac{1}{3}}\langle r|\varphi\rangle.$$

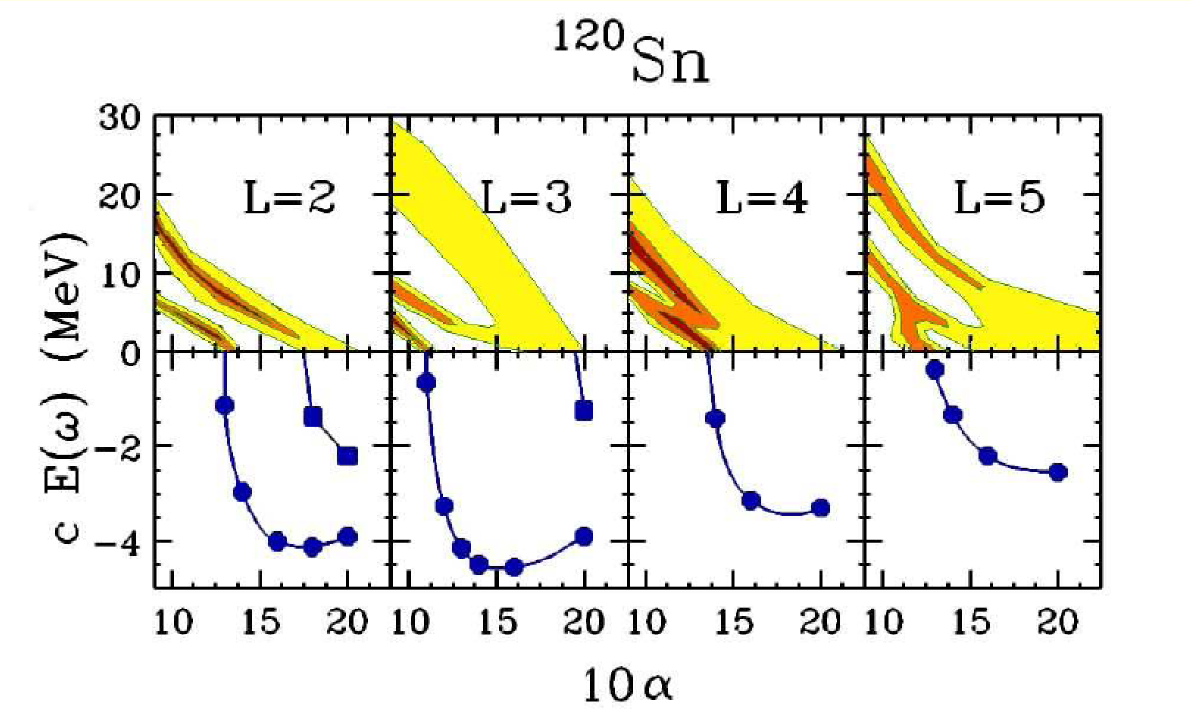

Collective modes
YLM(θ,φ)

Instabilities in nuclei

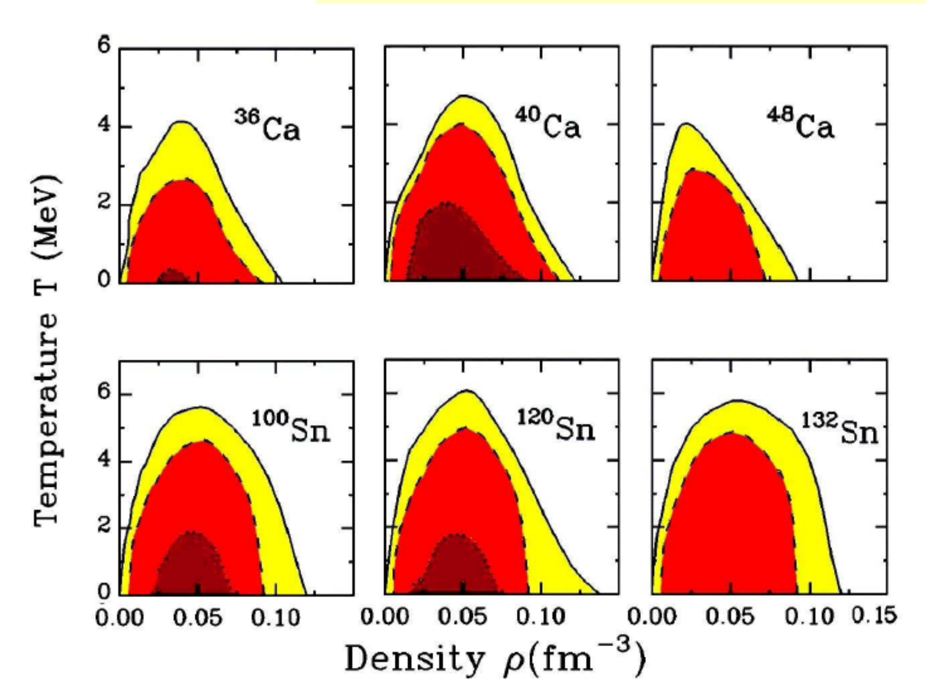

The role of charge asymmetry
(neutron-rich systems)

Isospin distillation in nuclei

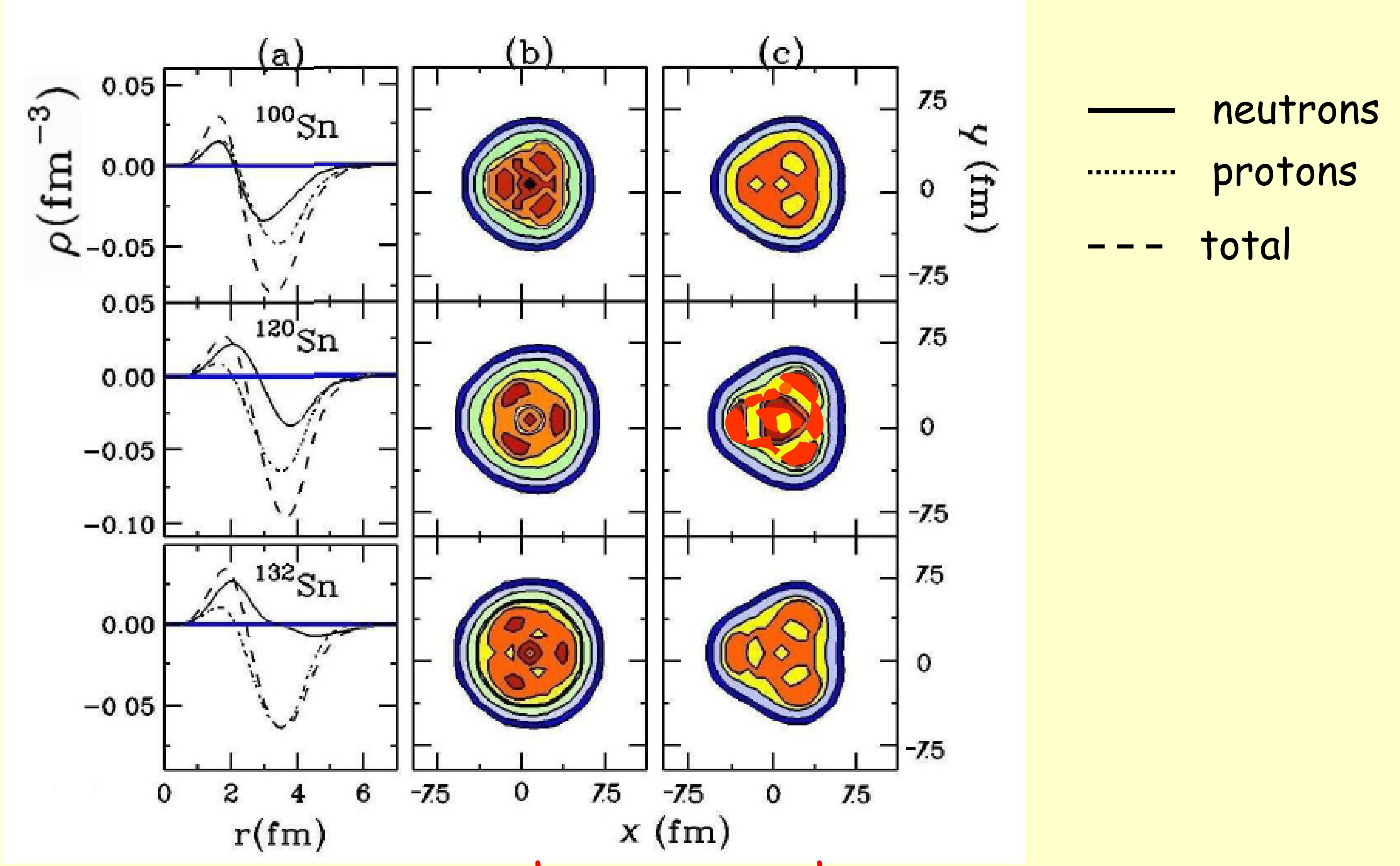

neutrons protons

Landau-Vlasov (BUU-BNV) equation

$$\dot{f} \equiv \frac{\partial}{\partial t} f - \{h[f], f\} = K[f] = \bar{K}[f] + \delta K[f]$$

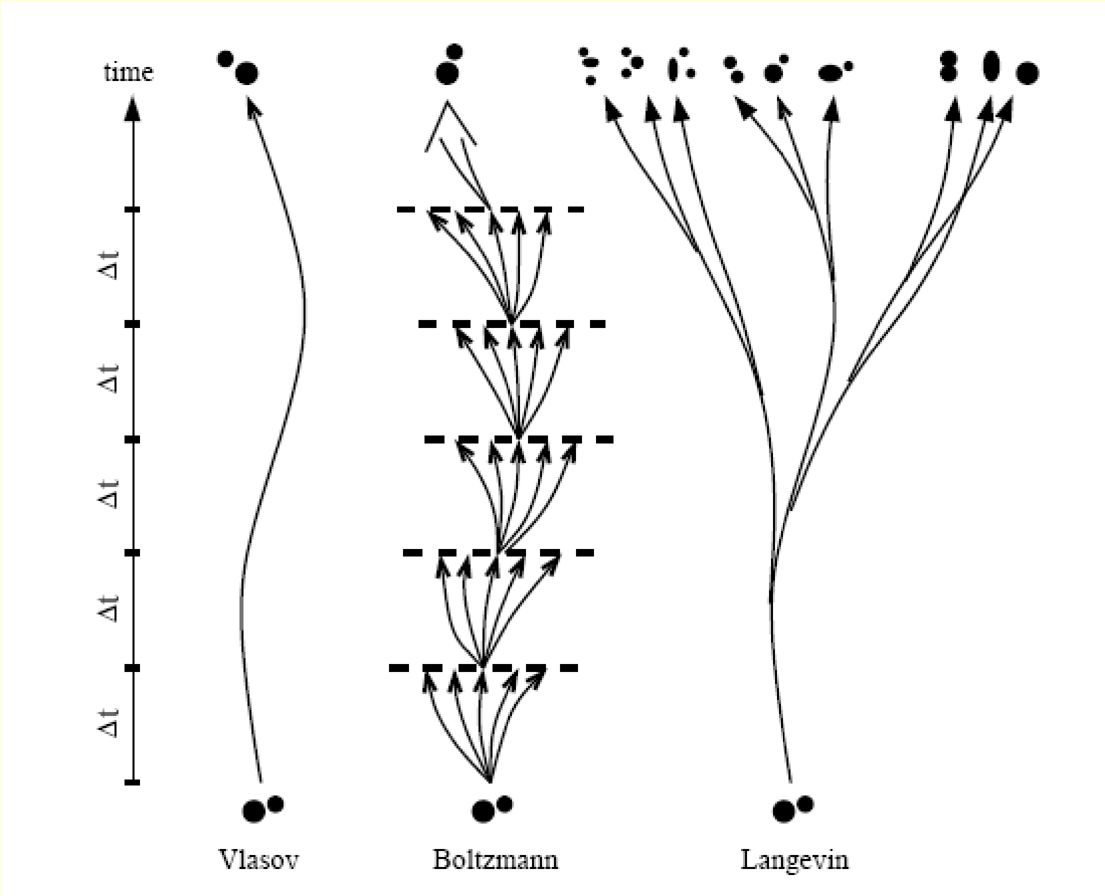

Boltzmann-Langevin (BL) equation

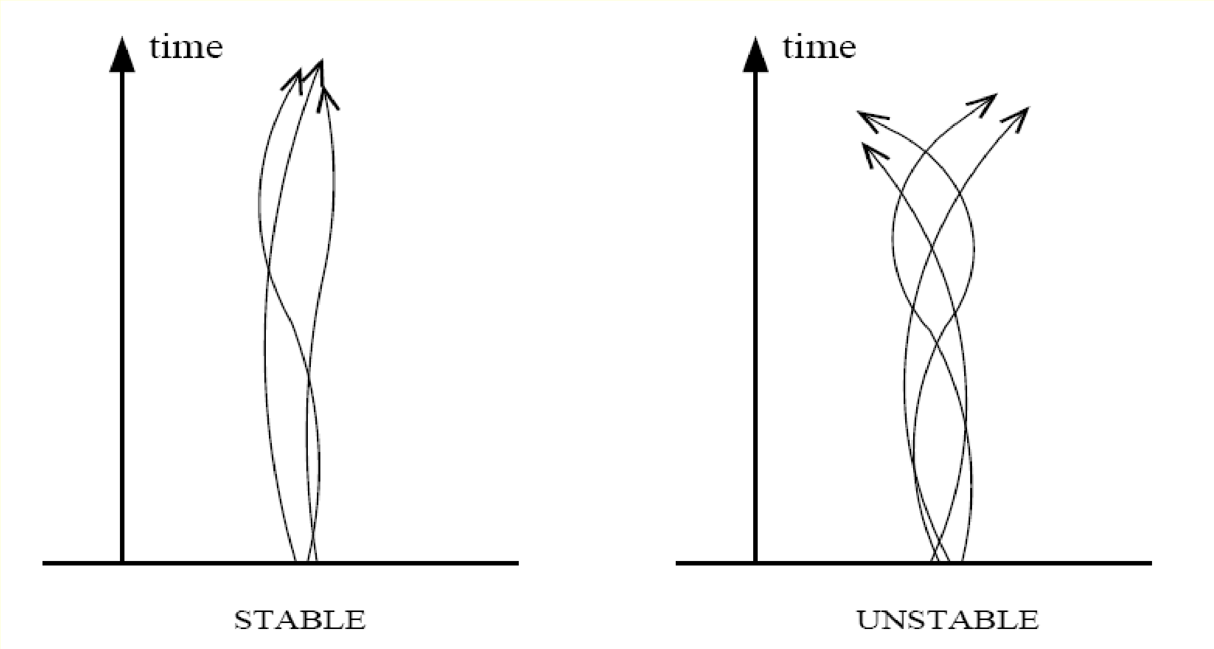

Effect of instabilities on trajectories

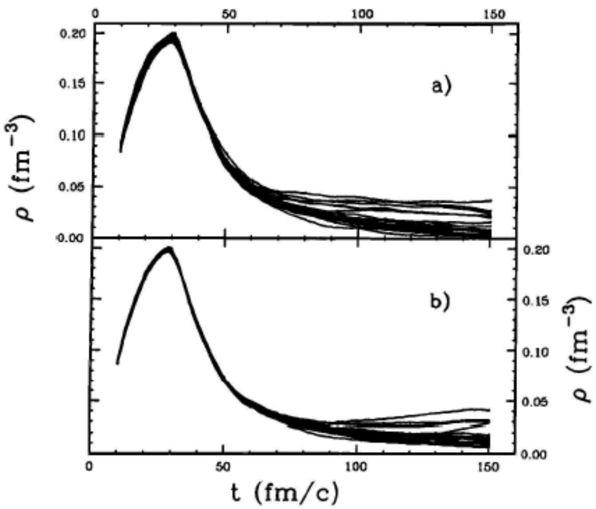

Figure 4-6: Effect of instabilities on the trajectory bundle.
The central density ρ as a function of time for 70 MeV/A Ca + Ca for bundles of dynamical trajectories resulting from different initial placings of $\mathcal{N}$ pseudo particles per nucleon, with either $\mathcal{N} = 40$ (a) or $\mathcal{N} = 100$ (b). (From Ref. [196].)

$$\bar{K}(\boldsymbol{r},\boldsymbol{p}_1) = g\sum_{234} W(12;34)\left[\bar{f}_1\bar{f}_2 f_3 f_4 - f_1 f_2 \bar{f}_3\bar{f}_4\right]$$

$$W(12;34) = v_{12}\left(\frac{d\sigma}{d\Omega}\right)_{12\to 34}\delta(\boldsymbol{p}_1+\boldsymbol{p}_2-\boldsymbol{p}_3-\boldsymbol{p}_4)$$

$$\prec \delta K(\boldsymbol{r},\boldsymbol{p},t)\ \delta K(\boldsymbol{r}',\boldsymbol{p}',t') \succ = C(\boldsymbol{p},\boldsymbol{p}',\boldsymbol{r},t)\ \delta(\boldsymbol{r}-\boldsymbol{r}')\ \delta(t-t')$$

$$\begin{aligned} C(\boldsymbol{p}_a,\boldsymbol{p}_b,\boldsymbol{r},t) &= \delta_{ab}\sum_{234} W(a2;34)F(a2;34) \\ &+ \sum_{34}\left[W(ab;34)F(ab;34) - 2W(a3;b4)F(a3;b4)\right] \end{aligned}$$

$\delta_{ab} \equiv h^3\delta(\boldsymbol{p}_a - \boldsymbol{p}_b)$ and $F(12;34) \equiv f_1 f_2 \bar{f}_3\bar{f}_4 + \bar{f}_1\bar{f}_2 f_3 f_4$.

$$\begin{aligned} \sum_1 C(\boldsymbol{p}_1,\boldsymbol{p}_2,\boldsymbol{r},t) &= \sum_2 C(\boldsymbol{p}_1,\boldsymbol{p}_2,\boldsymbol{r},t) &= 0 \\ \sum_1 C(\boldsymbol{p}_1,\boldsymbol{p}_2,\boldsymbol{r},t)\boldsymbol{p}_1 &= \sum_2 C(\boldsymbol{p}_1,\boldsymbol{p}_2,\boldsymbol{r},t)\boldsymbol{p}_2 &= \boldsymbol{0} \\ \sum_1 C(\boldsymbol{p}_1,\boldsymbol{p}_2,\boldsymbol{r},t)\epsilon_1 &= \sum_2 C(\boldsymbol{p}_1,\boldsymbol{p}_2,\boldsymbol{r},t)\epsilon_2 &= 0 \end{aligned}$$

Fluctuation correlations

Linearization of BL equation

$$\frac{\partial}{\partial t}\delta f = -i\mathcal{M}[f_0]\delta f + \delta K[f_0]$$

$$\delta f(\mathsf{s},t) = \sum_\nu A_\nu(t) f_\nu(\mathsf{s})$$

$$A_\nu(t) = \mathrm{e}^{-i\omega_\nu t}\left(A_\nu(0) + \int_0^t dt'\ B_\nu(t')\ \mathrm{e}^{i\omega_\nu t'}\right)$$

$$B_\nu(t) = \sum_\mu O_{\nu\nu'}\langle f_\mu\,;\delta K(t)\rangle$$

O^{-1} overlap matrix

$$\prec B_\nu(t)B_\mu(t')^* \succ = 2\mathcal{D}_{\nu\mu}\,\delta(t-t')$$

$$\mathcal{D}_{\nu\mu} = \sum_{\nu'\mu'} O_{\nu\nu'}\Delta_{\nu'\mu'}O_{\mu'\mu}$$

$$\Delta_{\nu\mu} = \langle f_\nu\,;D\ f_\mu\rangle = \int d\mathsf{s}\int d\mathsf{s}'\ f_\nu(\mathsf{s})^* D(\mathsf{s};\mathsf{s}')f_\mu(\mathsf{s}')$$

$$= \frac{1}{2}\int dv_{12;34}\,\{f_\nu(1)^*\,[f_\mu(1)+f_\mu(2)-2f_\mu(1')] + f_\nu(1')^*\,[f_\mu(1')+f_\mu(2')-2f_\mu(1)]\}\,.$$

$$\frac{d}{dt}\sigma_{\nu\mu} = -i\omega_{\nu\mu}\sigma_{\nu\mu} + 2\mathcal{D}_{\nu\mu}$$

$$\sigma_{\nu\mu}(t) = -i\frac{2\mathcal{D}_{\nu\mu}}{\omega_{\nu\mu}}\left(1 - \mathrm{e}^{-i\omega_{\nu\mu}t}\right) + \sigma_{\nu\mu}(0)\,\mathrm{e}^{-i\omega_{\nu\mu}t}.$$

$$\sigma_{\nu\nu}(t) = \begin{cases} \mathcal{D}_\nu^{\mathrm{var}} t_\nu \left(1 - \mathrm{e}^{-2t/t_\nu}\right) + \sigma_{\nu\nu}(0)\mathrm{e}^{-2t/t_\nu} & \rightarrow 2\mathcal{D}_\nu^{\mathrm{var}} t_\nu \\ \mathcal{D}_\nu^{\mathrm{var}} t_\nu \left(\mathrm{e}^{2t/t_\nu} - 1\right) + \sigma_{\nu\nu}(0)\mathrm{e}^{2t/t_\nu} & \rightarrow \left(2\mathcal{D}_\nu^{\mathrm{var}} t_\nu + \sigma_{\nu\nu}(0)\right)\mathrm{e}^{2t/t_\nu} \end{cases}$$

Development of fluctuations in presence of instabilities

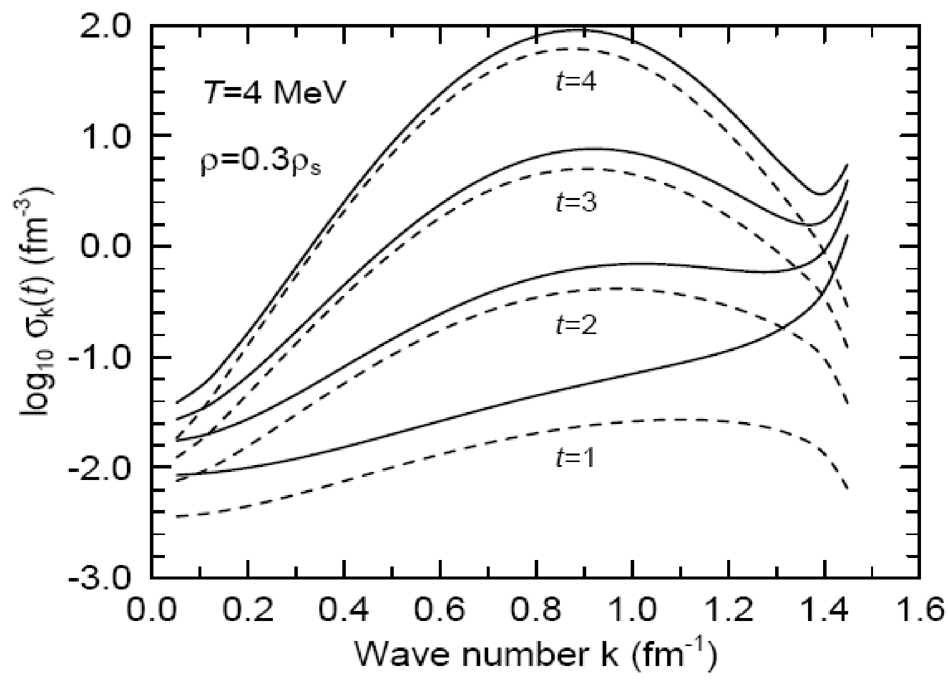

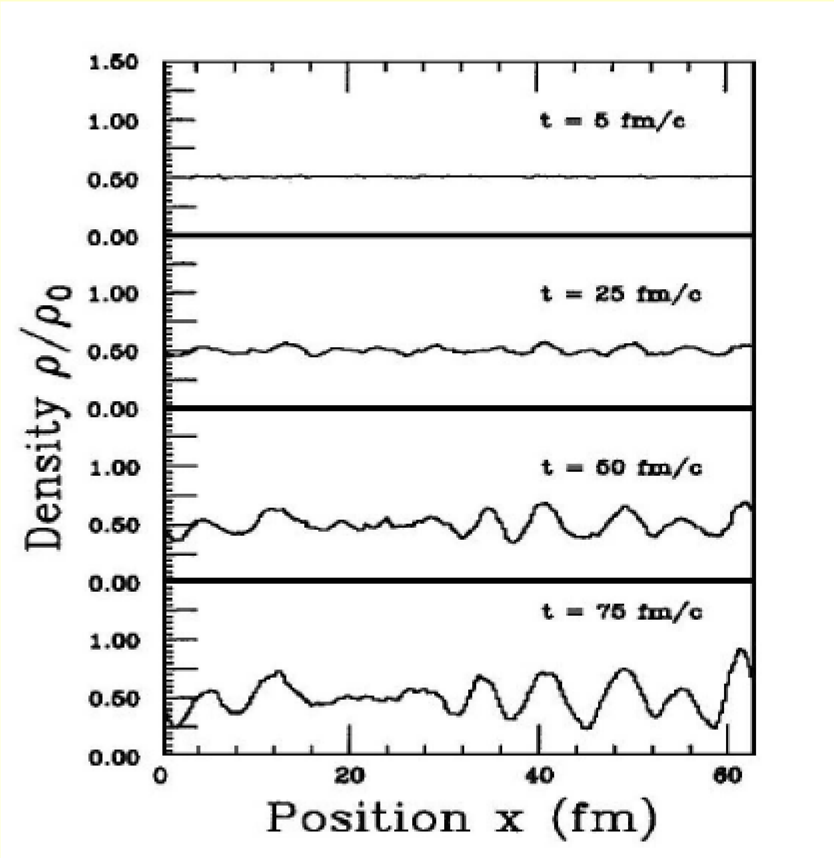

Fragment formation in BL treatment

Exponential increase

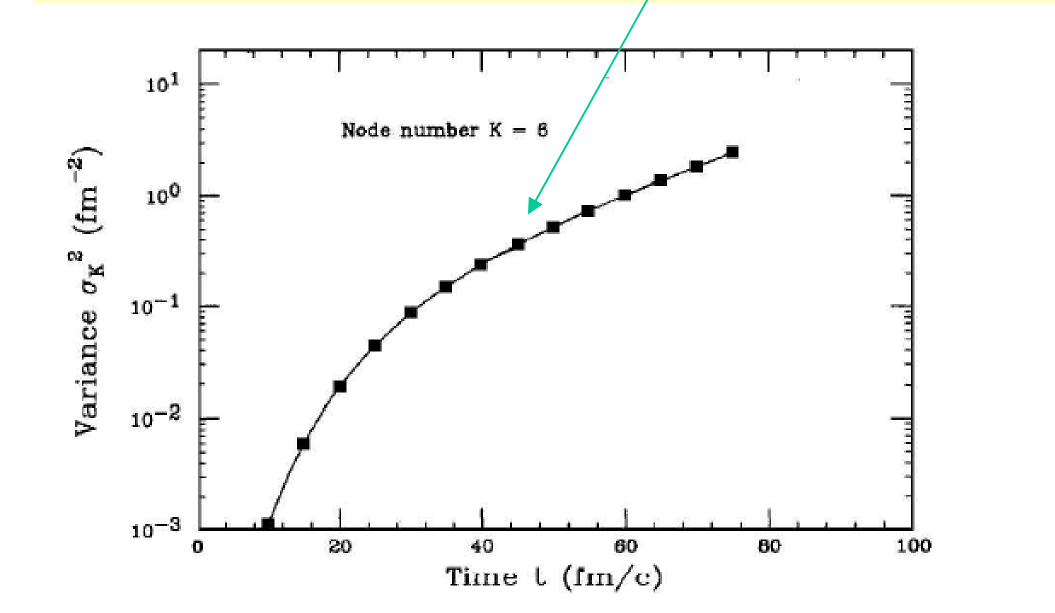

Growth of instabilities

Approximate BL treatment ---- BOB dynamics

$$\delta K[f] \rightarrow \delta \tilde{K}[f] = -\delta \boldsymbol{F} \cdot \frac{\partial f}{\partial \boldsymbol{p}} .$$

$$\prec \delta \boldsymbol{F}(\boldsymbol{r}_1)\, \delta \boldsymbol{F}(\boldsymbol{r}_2) \succ = 2\tilde{D}_0(\boldsymbol{r})\, \boldsymbol{I}\, \delta(\boldsymbol{r}_{12})\, \delta(t_{12})$$

$$2\tilde{D}(\mathsf{s}_1;\mathsf{s}_2) = 2\tilde{D}_0(\boldsymbol{r}) \frac{\partial f(\mathsf{s}_1)}{\partial \boldsymbol{p}_1} \cdot \frac{\partial f(\mathsf{s}_2)}{\partial \boldsymbol{p}_2} \delta(\boldsymbol{r}_{12}) .$$

(Brownian One Body, Stochastic Mean Field (SMF), …)

Growth of instabilities (comparison BL-BOB)

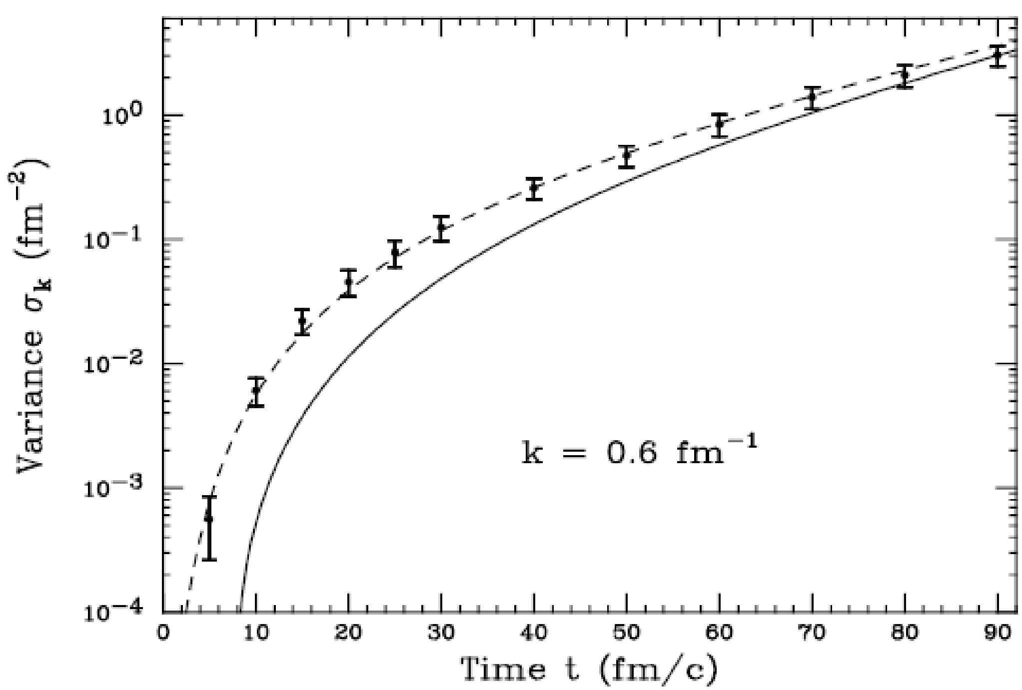

Applications to nuclear fragmentation

Some examples of reactions

Xe + Sn ,	E/A = 30 - 50 MeV/A
Sn + Sn,	50 MeV/A
Au + Au	30 MeV/A
p + Au	1 GeV/A
Sn + Ni	35 MeV/A

E*/A ~ 5 MeV , T ~ 3-5 MeV

LBL
MSU
Texas A&M
GANIL
GSI
LNS

Is the spinodal region attained in nuclear collisions ?

Some examples of trajectories as predicted by
Semi-classical transport equations (BUU)

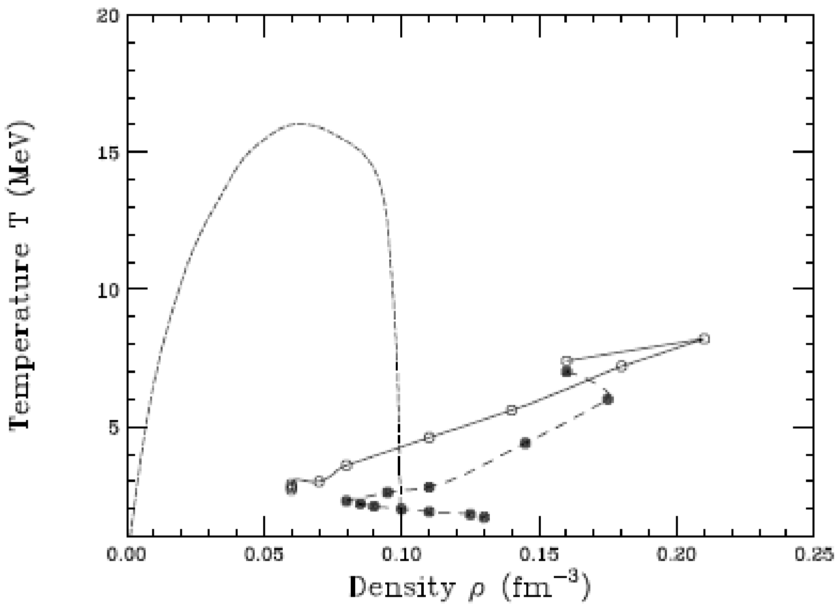

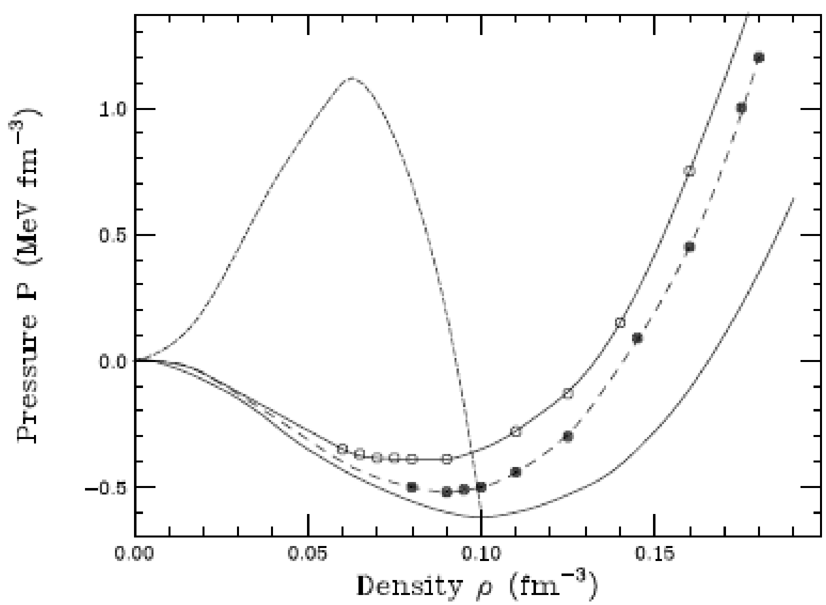

- ○ ***La + Cu 55 AMeV***
- ● ***La + Al 55 AMeV***

Expansion and dissipation in TDHF simulations:
both compression and heat are effective

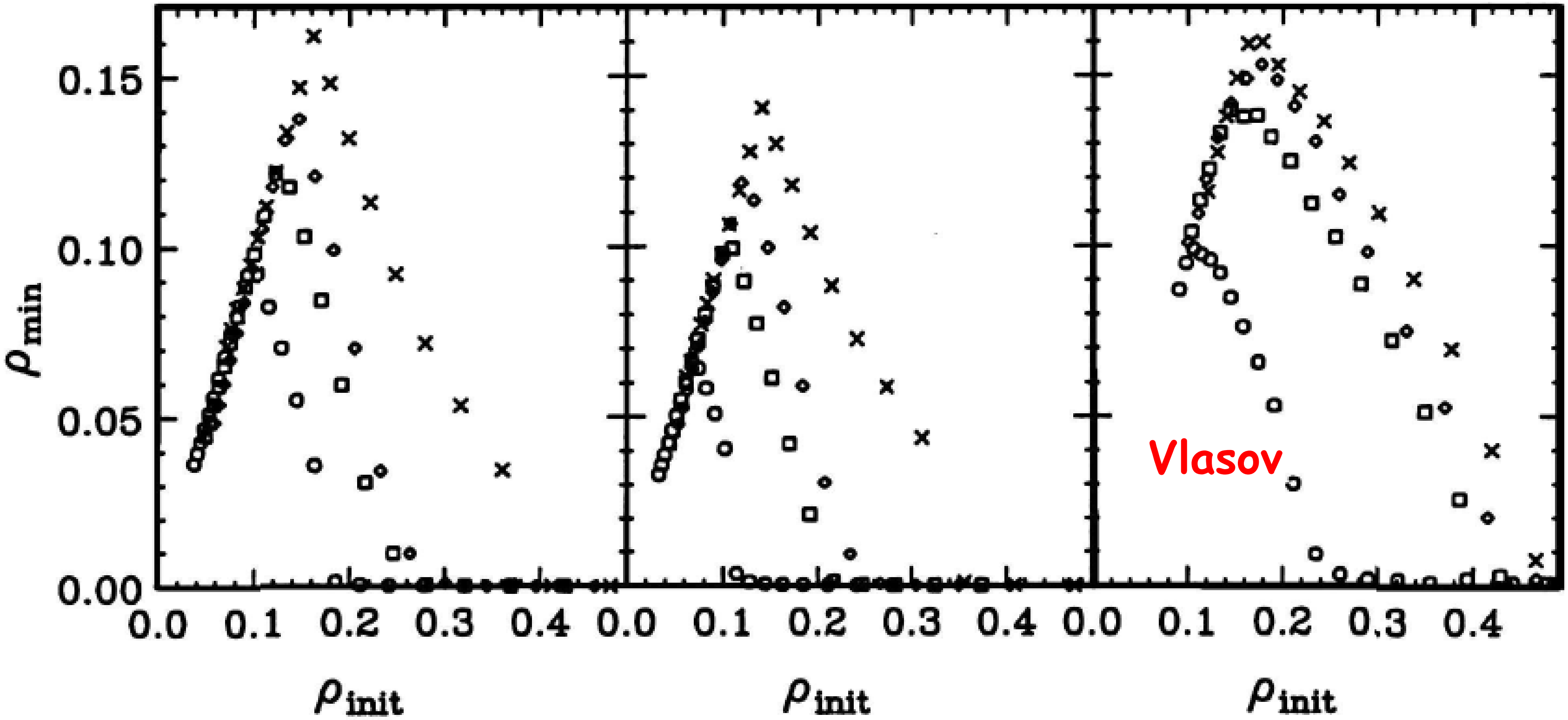

The central density at the time of maximum dilution (the turning point in the monopole motion), $\rho_{\rm min}$, as a function of the initial central density $\rho_{\rm init}$, for a ^{40}Ca nucleus at various initial temperatures, either in TDHF (left and center) and the corresponding Vlasov treatment (right). The initial excitations correspond to the following values of the entropy per nucleon σ: 0 (crosses), 1.1 (diamonds), 2.35 (squares) and 3.28 (circles) which correspond to $T = 0$, 5, 10 and 15 MeV for the uncompressed heated nuclei. (From Ref. [232].)

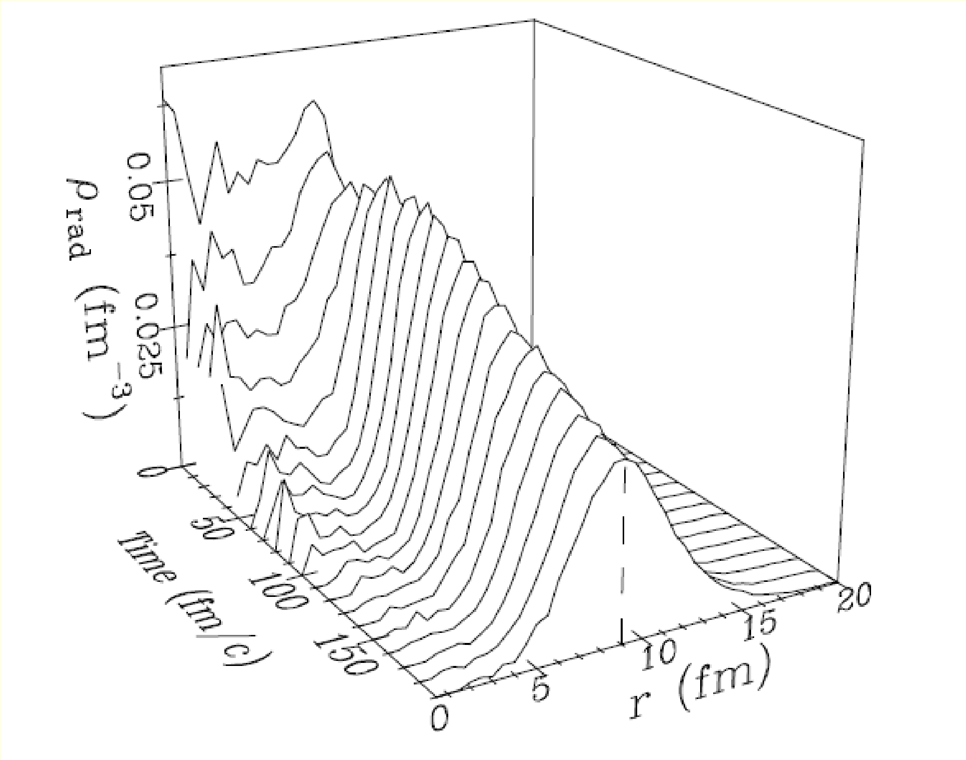

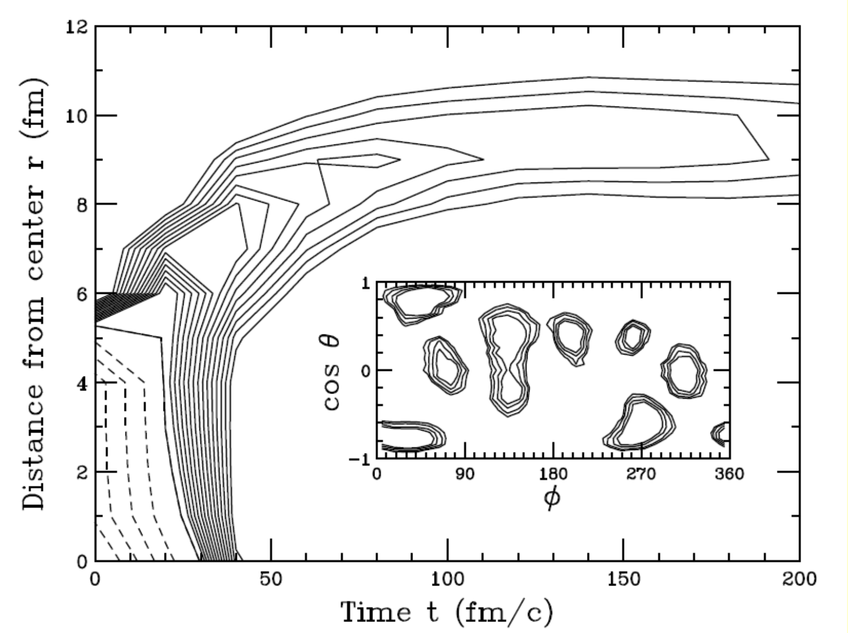

Stochastic mean-field
SMF (BL like) results

Expansion dynamics in presence of fluctuations

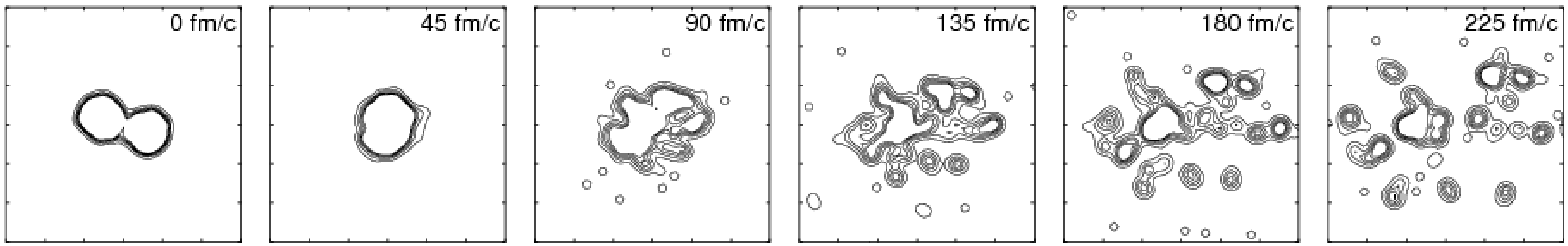

Compression and expansion in Antisymmetrized-Molecular Dynamics simulations (AMD)

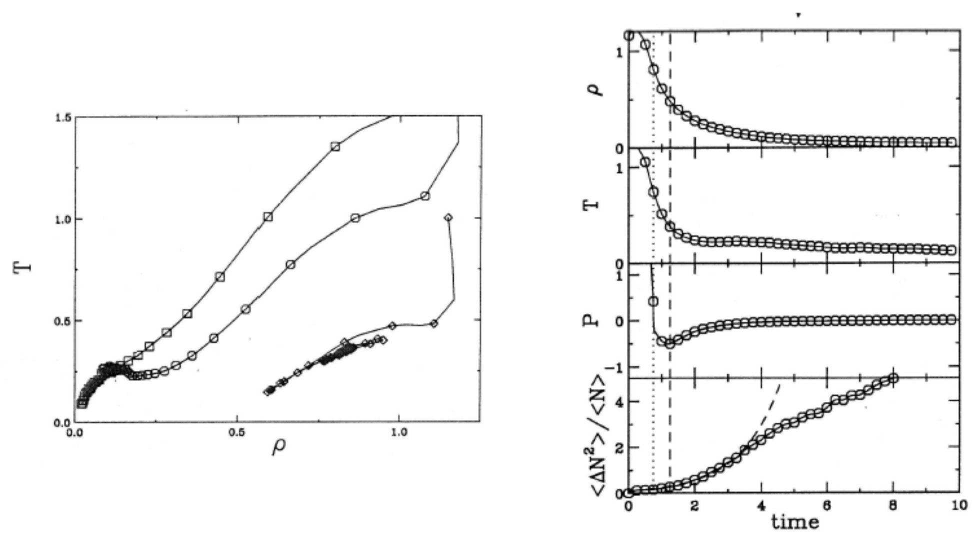

Figure 5-9: Fragmentation of a hot drop.
The time evolution of a hot spherical assembly of N interacting particles. *Left:* Trajectories followed the $T-\rho$ phase plane for the three energies considered and $N = 251$ (see text). *Right:* Time evolution of pressure, density, temperature and multiplicity fluctuations obtained in the case yielding maximum IMF production ($N = 485$). (From Ref. [77].)

Thermal expansion in MD (classical) simulations

Fragmentation studies

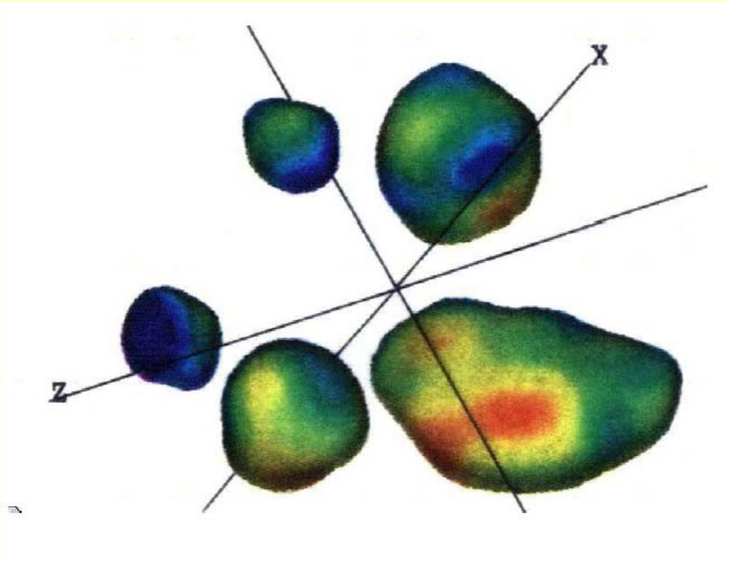

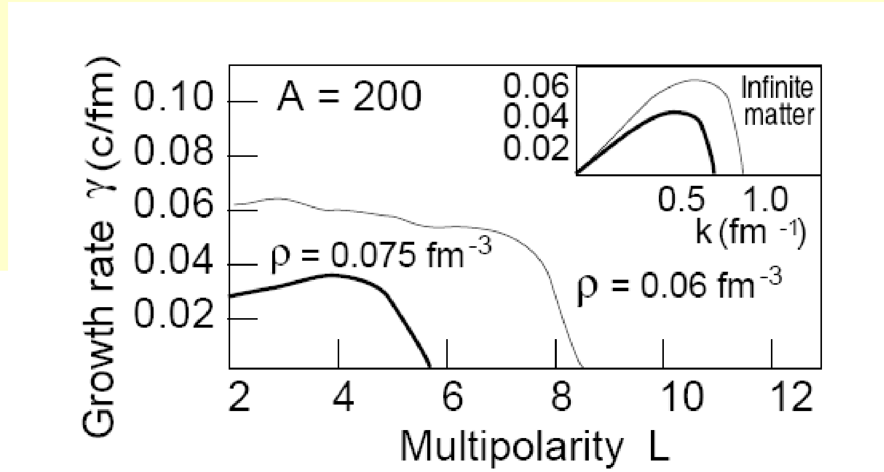

RPA predictions

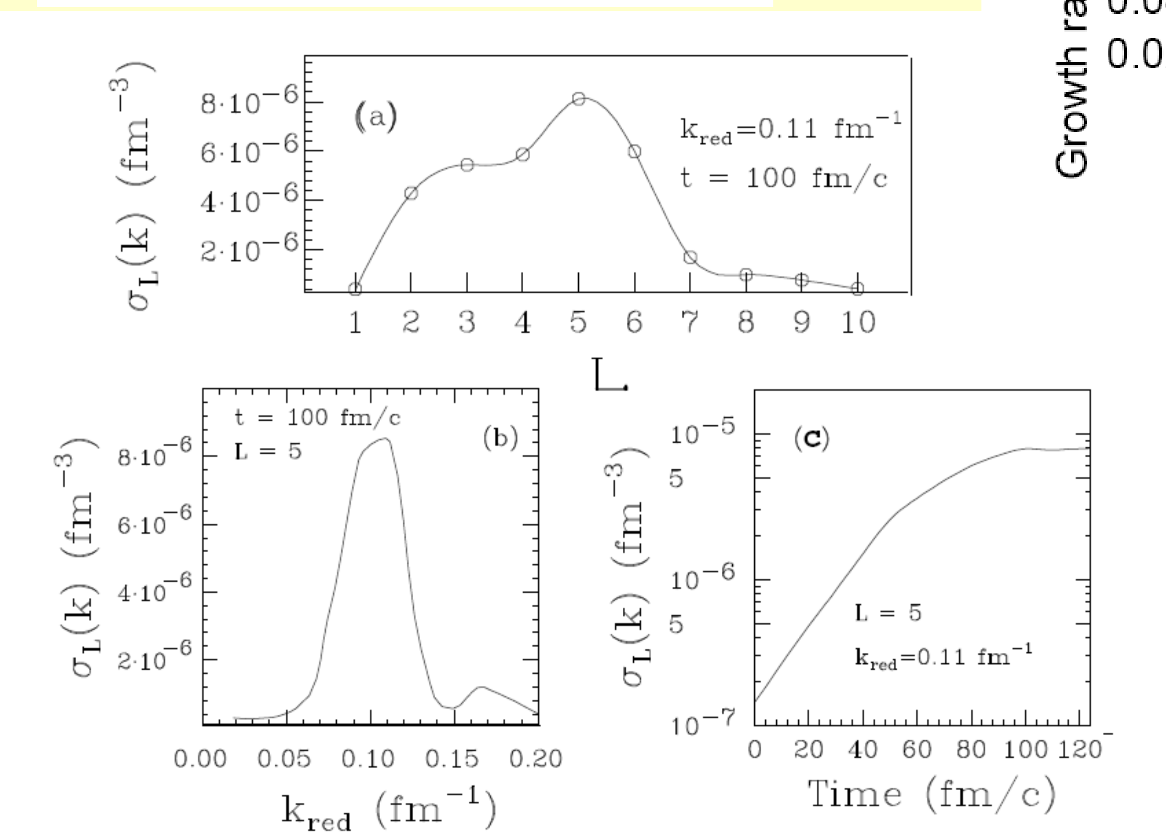

SMF calculations

Fragment reconstruction

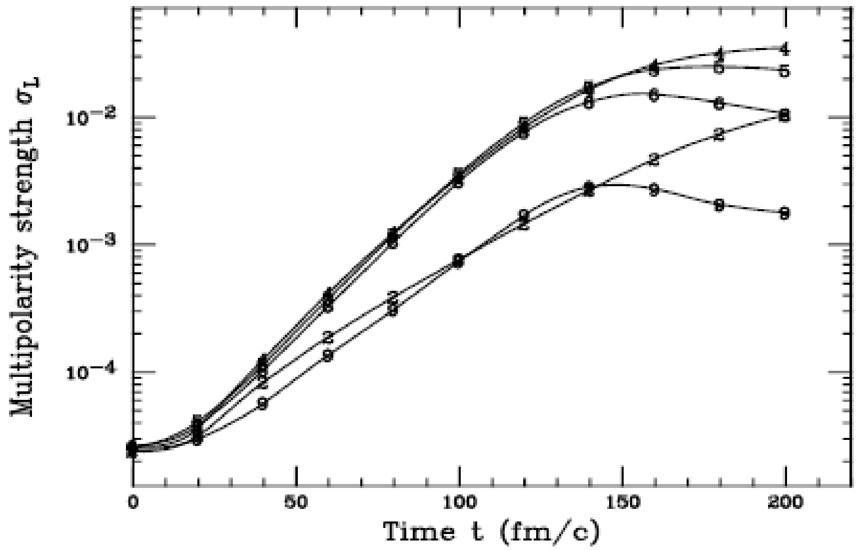

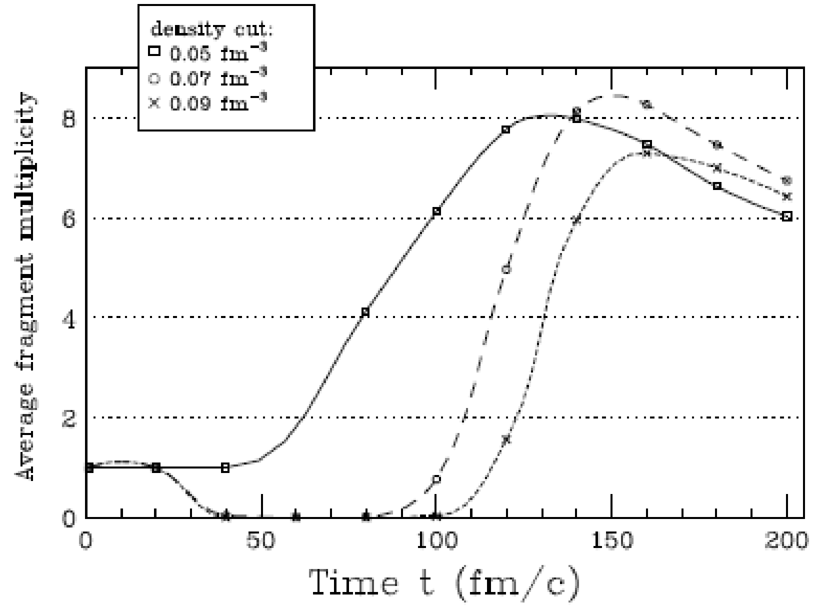

Experimental observables :
IMF multiplicity,
charge distributions,
Kinetic energies,
IMF-IMF correlations …

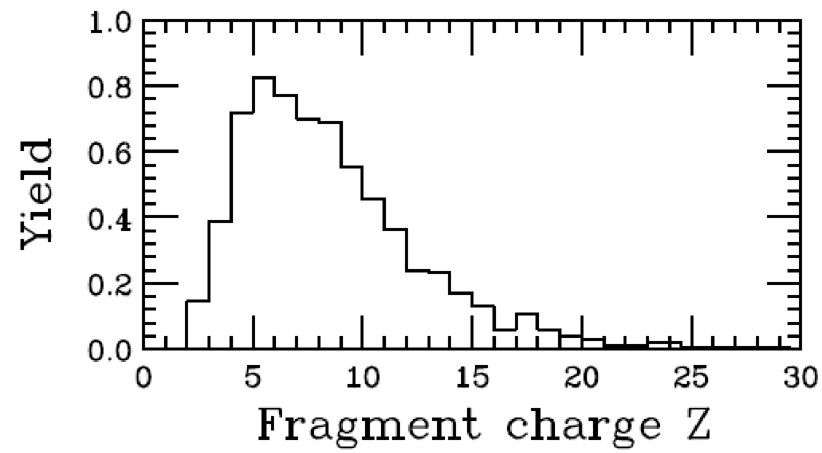

Confrontation with experimental data

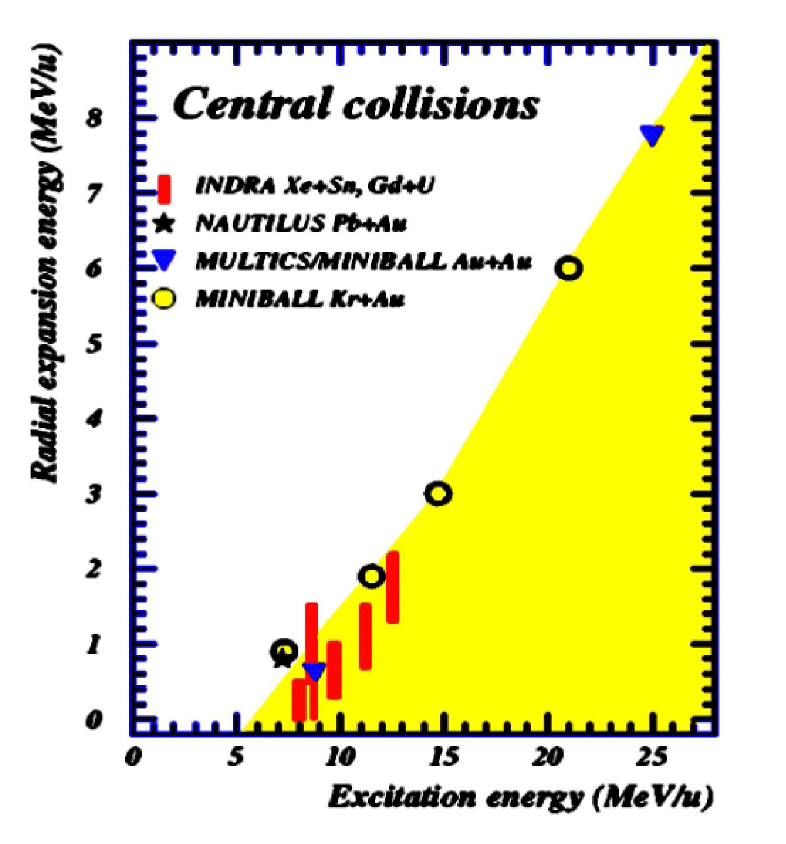

Compilation of experimental data on radial flow
Onset of nuclear explosion around 5-7 MeV/u

p + Au

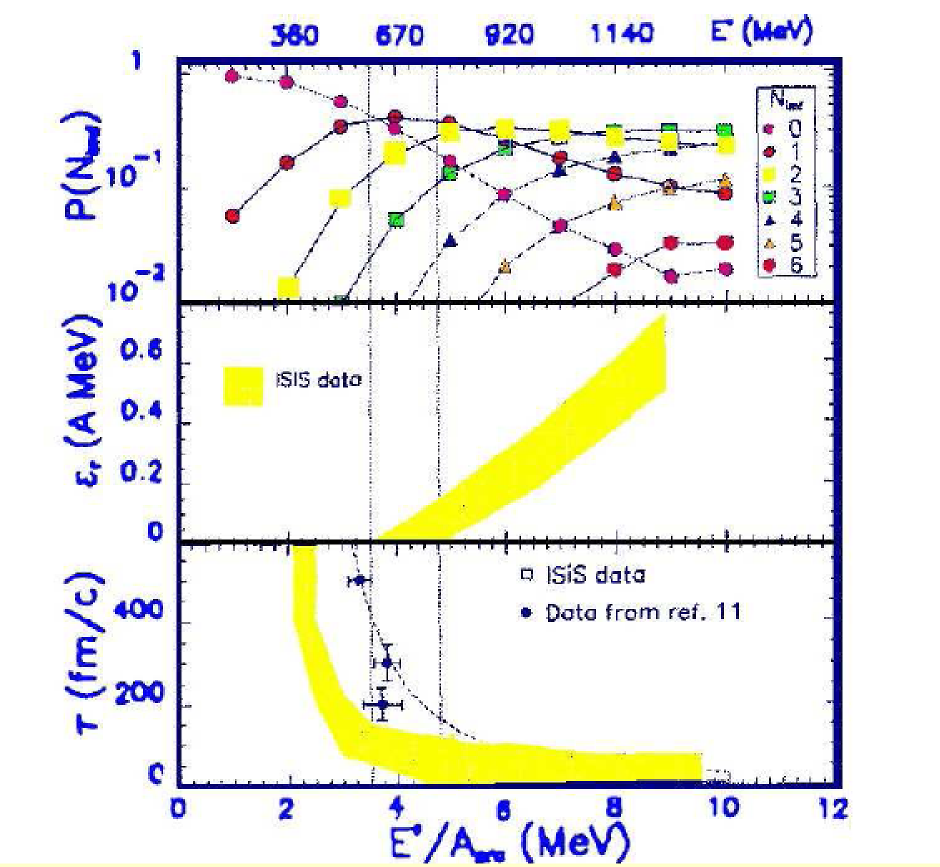

From two-fragment correlation Function ⟶
Fragment emission time
Onset of radial expansion
IMF emission probability

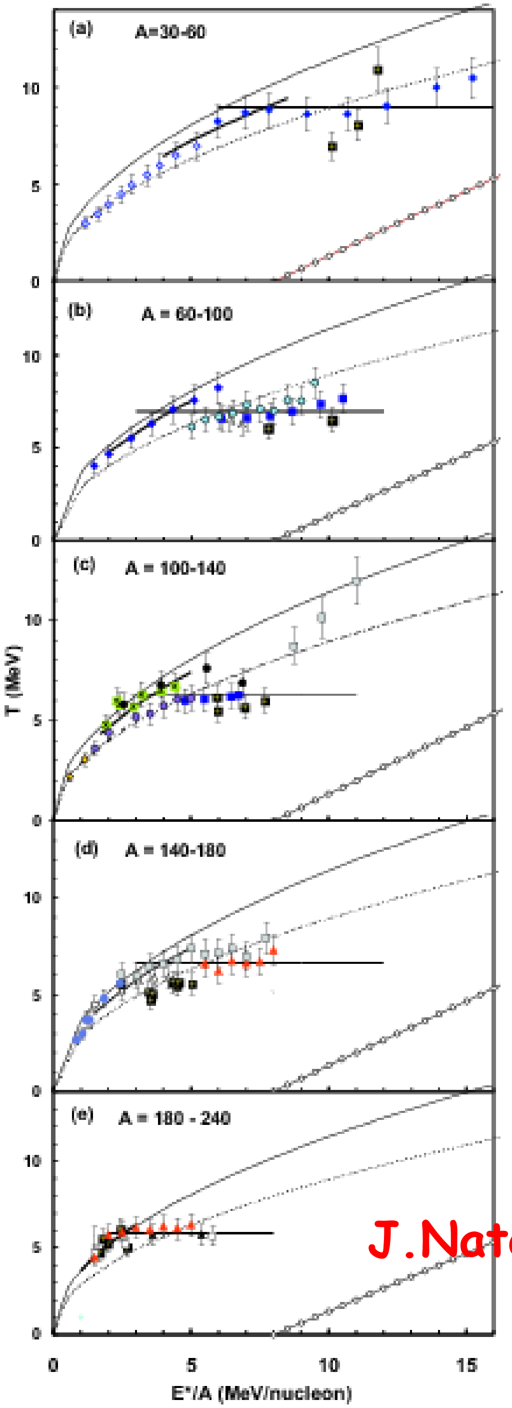

J.Natowitz et al.

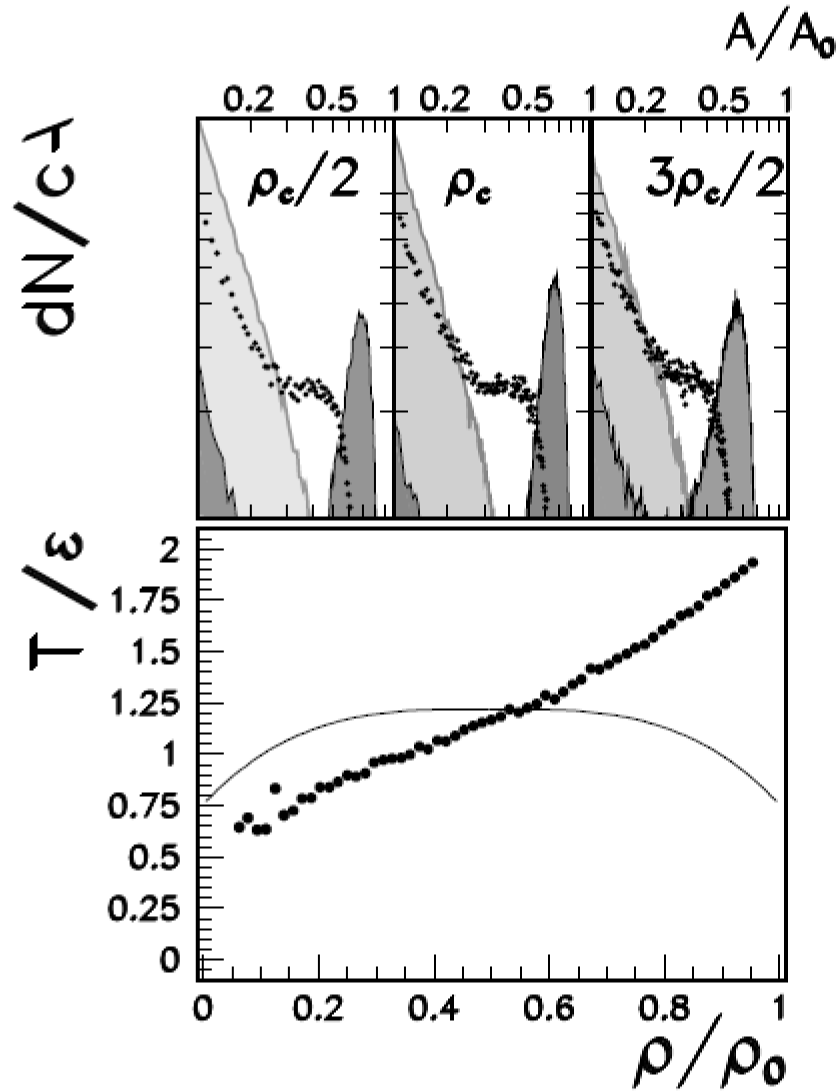

Lattice-gas calculations

Nuclear caloric curves and critical behaviour

Further evidences of multifragmentation as a process happening inside the co-existence zone

Kinetic energy fluctuations

Negative specific heat

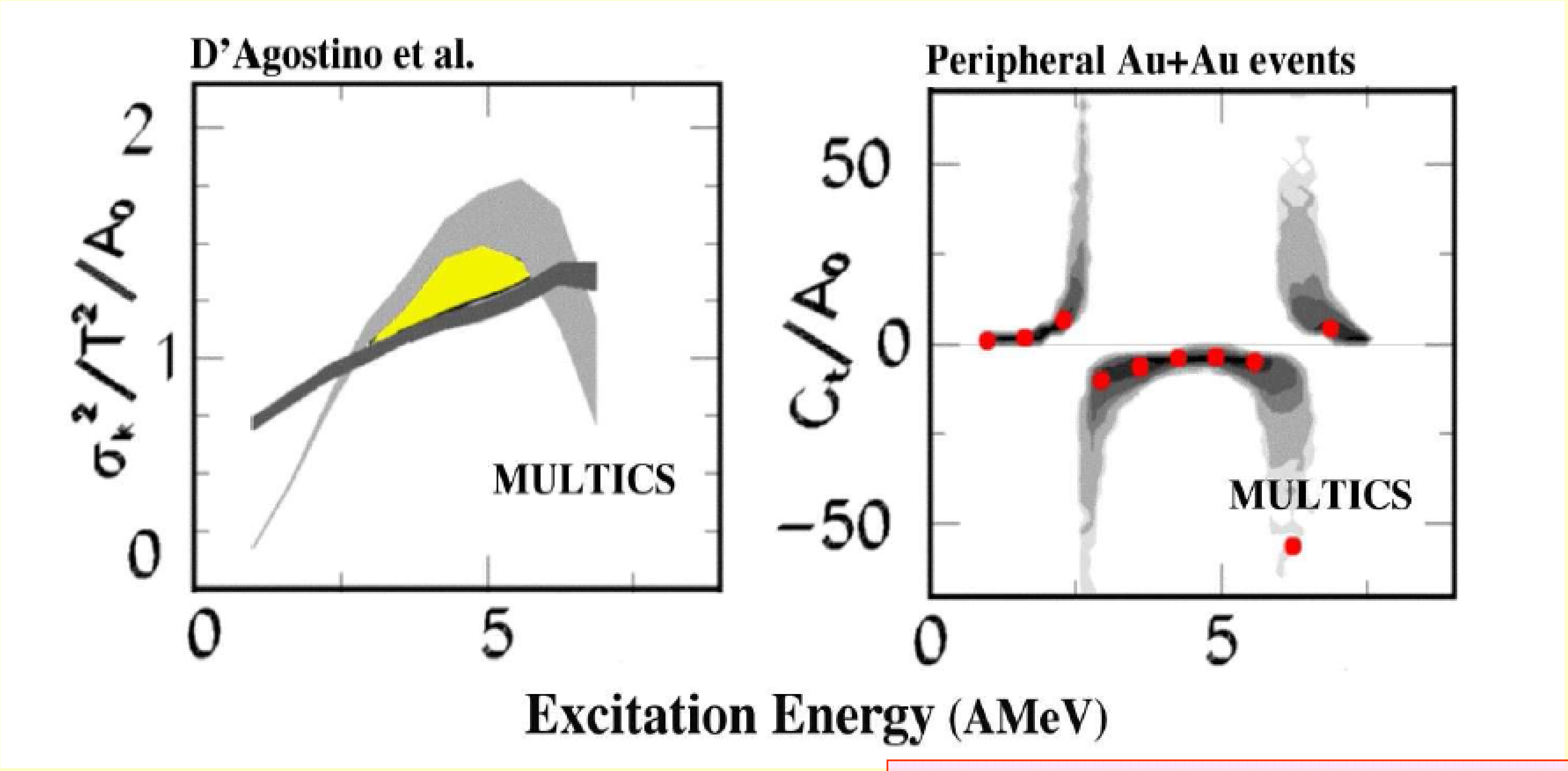

M.D'Agostino et al., NPA699(2002)795

Comparison with the INDRA data: central reactions

Largest fragment distribution

Charge distribution

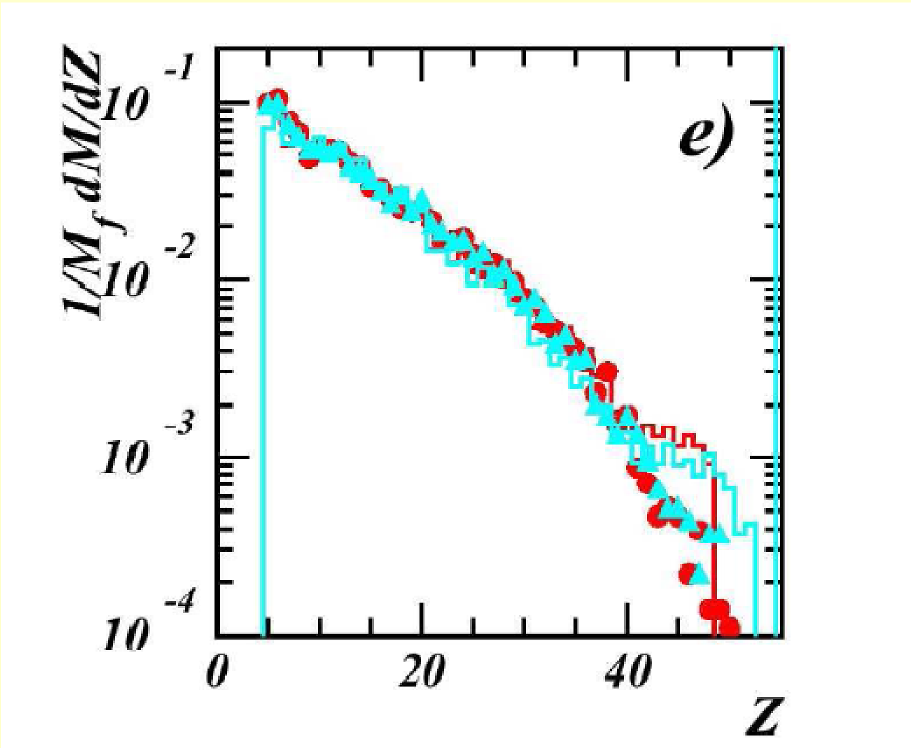

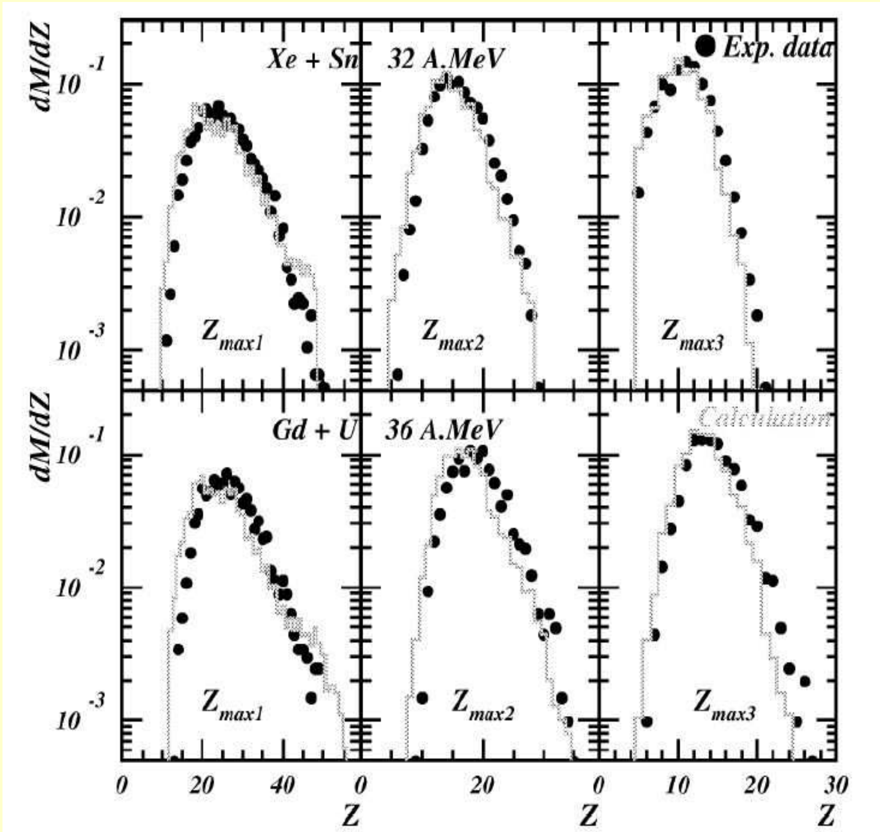

Fragment kinetic energies :
Comparison between calculations and data

Uncertainties ………
Pre-equilibrium emission
Exc.energy estimation
Impact parameter
Ground state …..

But typical shape well reproduced !

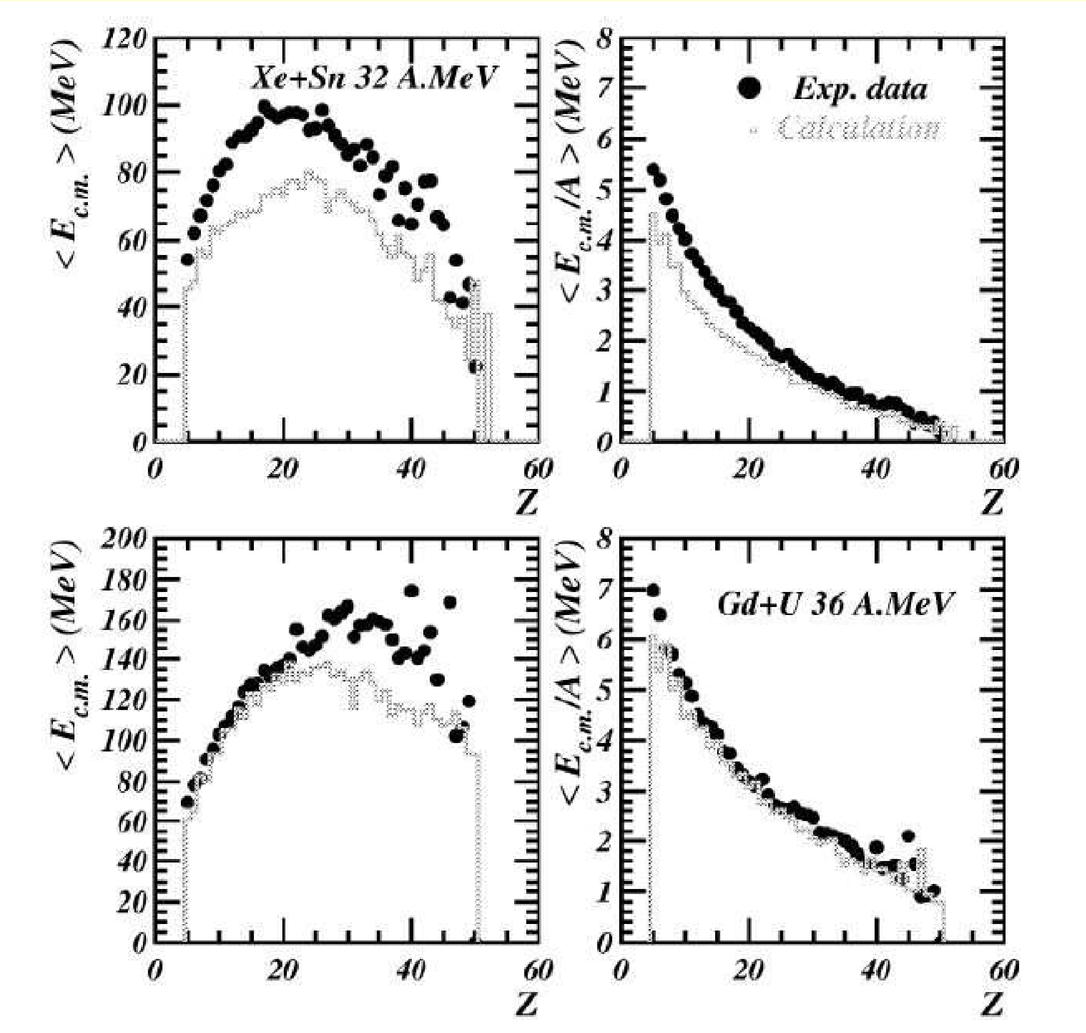

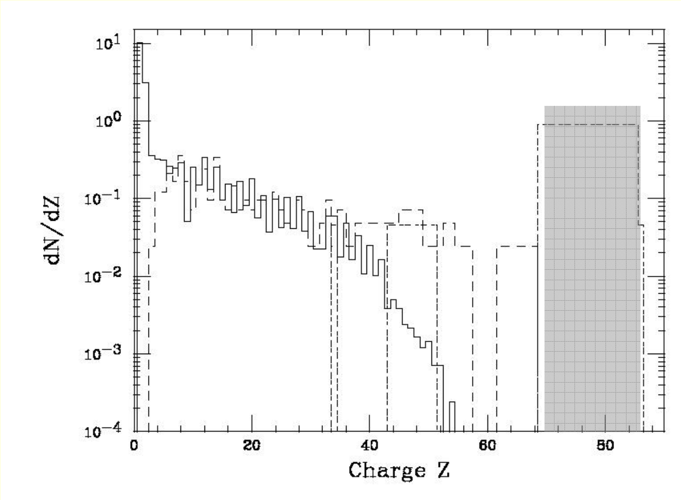

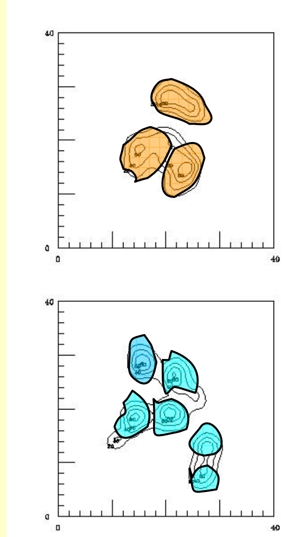

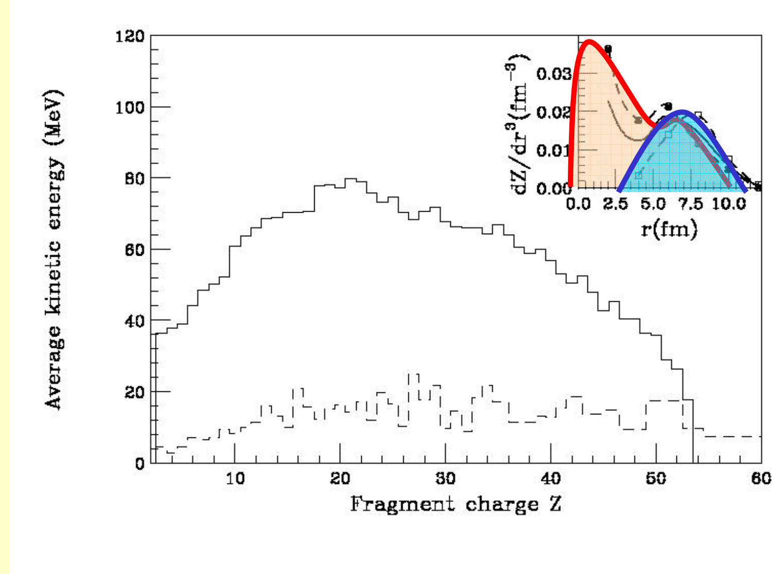

^{129}Xe + ^{119}Sn   32 AMeV

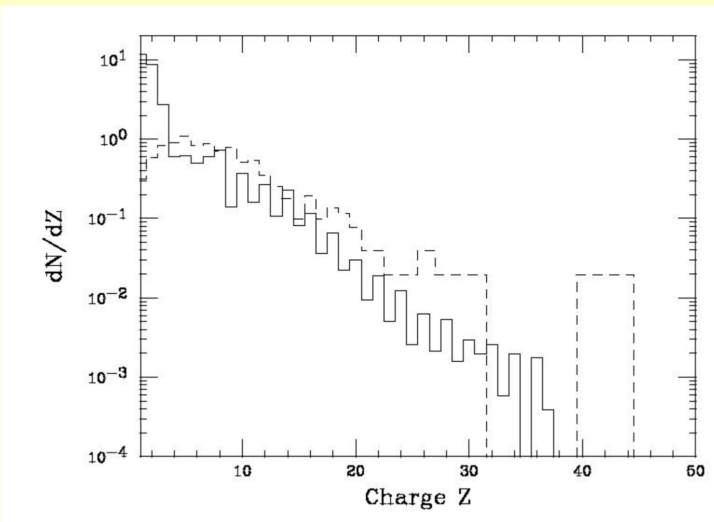

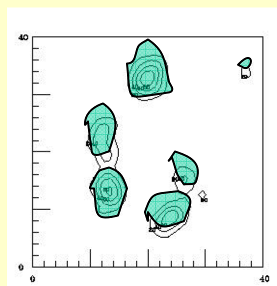

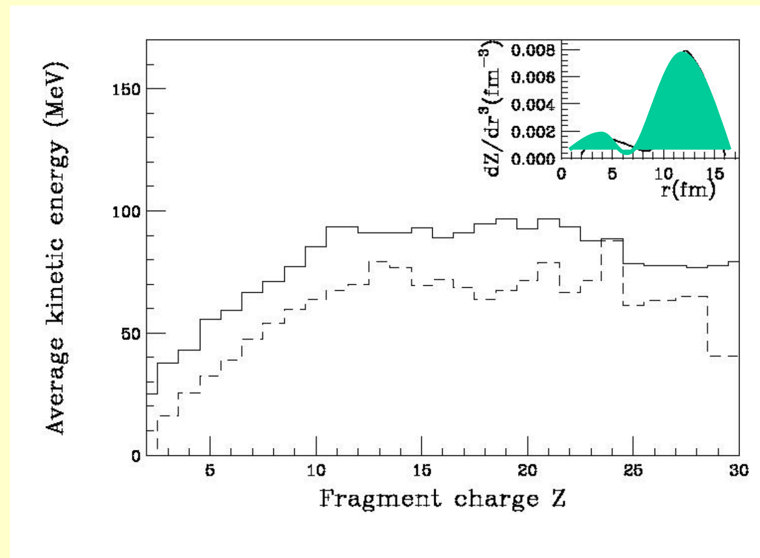

^{129}Xe + ^{119}Sn   50 AMeV

Event topology

A more sophisticated analysis:
IMF-IMF velocity correlations

Event topology:

Structure of fragments at freeze-out:

Uniform distribution or bubble-like shape ?

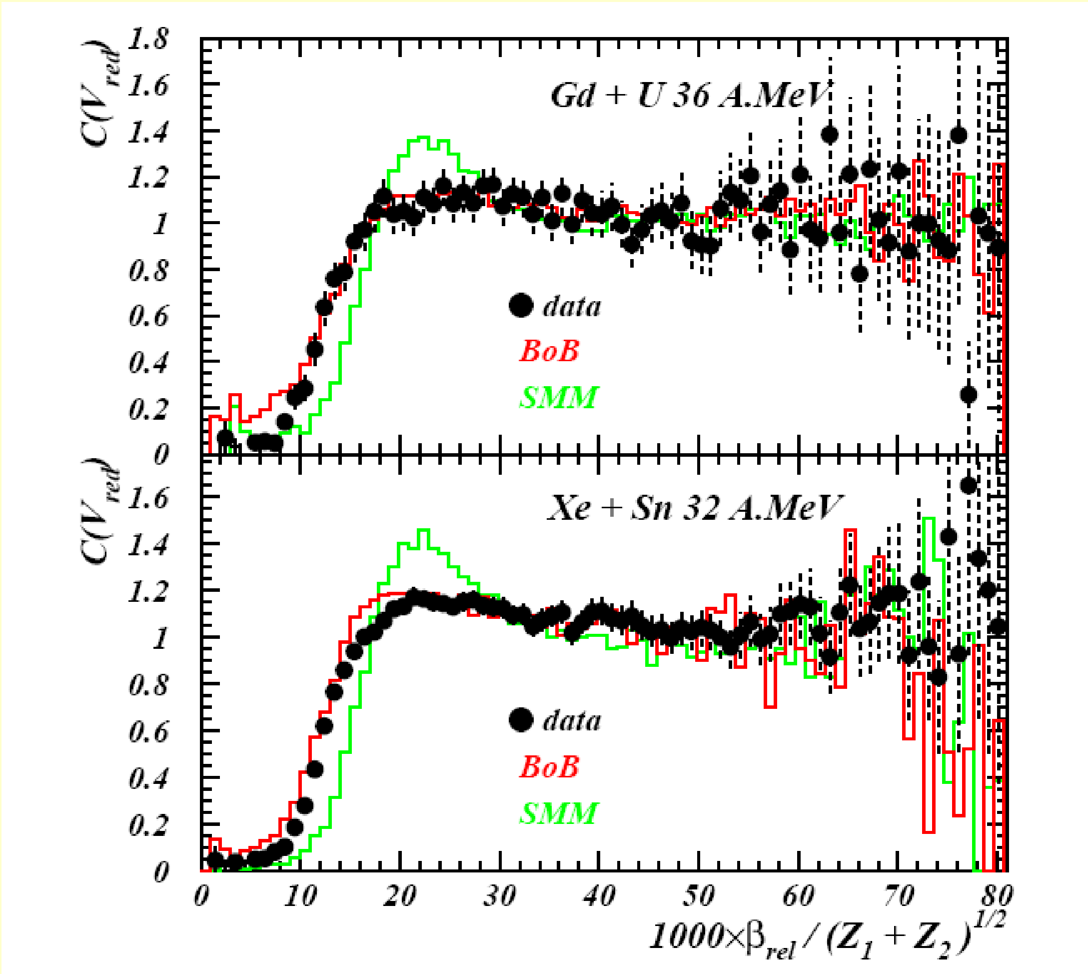

Fragment size correlations

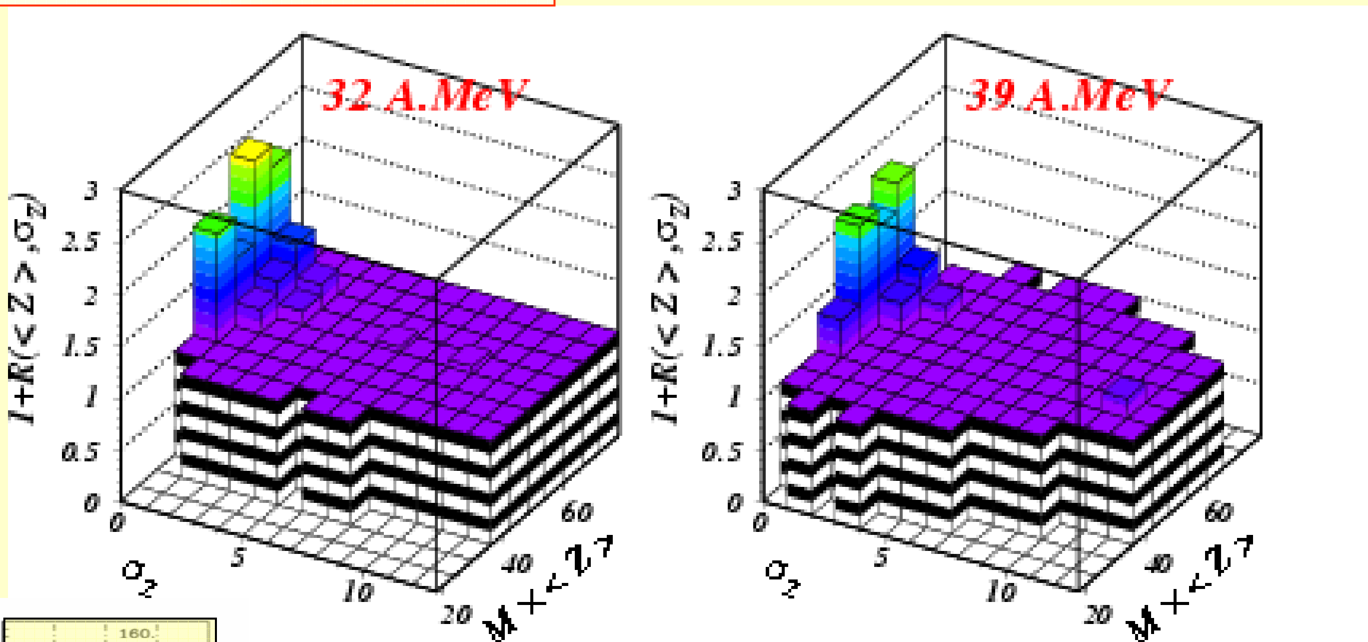

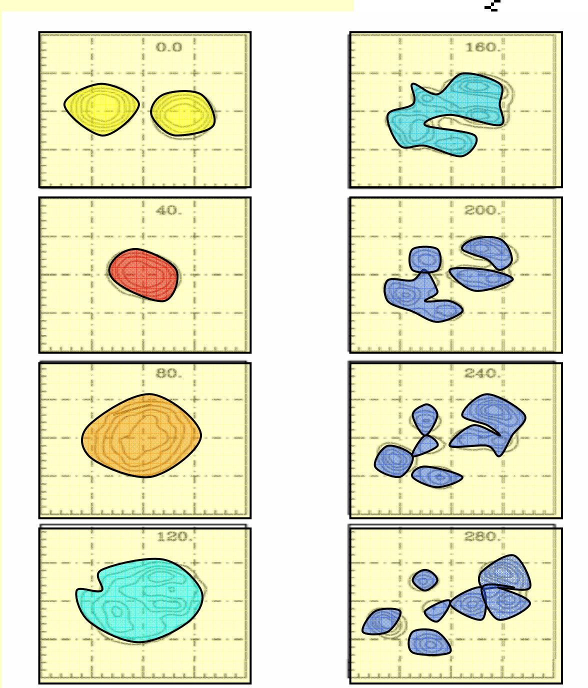

For each event: ‹Z›, ΔZ

ΔZ ⟶ 0 Relics of equal size fragment partitions !

Relics of spinodal instabilities:
Events with equal-size fragments
G.Tabacaru et al., EPJA18(2003)103

Spinodal decomposition in other fields

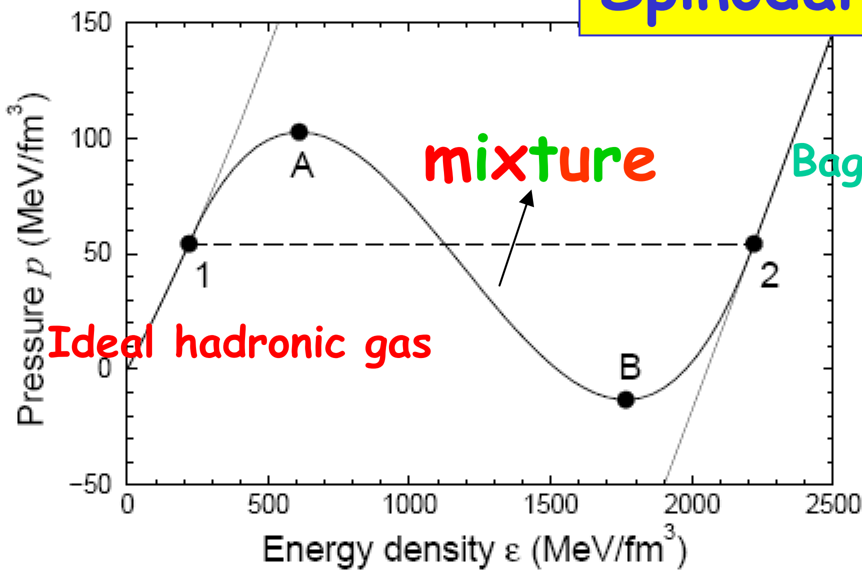

Bag with quarks and nucleons

QGP

Onset of spinodal decomposition:
development of characteristic patterns in ε (azimuthal multipolarity) →

Influence on flow coefficients

$$\partial_t^2 \delta\varepsilon(t,r) = \frac{\partial p_0}{\partial \varepsilon_0} \nabla^2 \delta\varepsilon(t,r) .$$

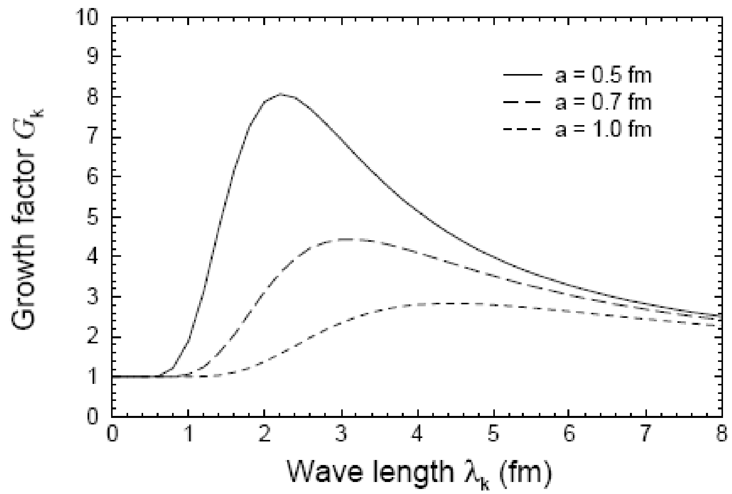

J.Randrup, PRL92(2004)122301

Neutron stars

✓In the outer part of the star, (stellar crust), densities are similar to nuclear case.
Star modelized in terms of n,p, e,ν.

✓Evolution of the crust during the cooling process.